

Probabilistic Roadmaps for Aerial Relay Path Planning

Pham Q. Viet and Daniel Romero

Dept. of Information and Communication Technology, University of Agder, Grimstad, Norway.

Email: {viet.q.pham,daniel.romero}@uia.no.

Abstract—Autonomous unmanned aerial vehicles (UAVs) can be utilized as aerial relays to serve users far from terrestrial infrastructure. Existing algorithms for planning the paths of multiple aerial relays cannot generally accommodate flight constraints. These are imposed by the presence of obstacles, such as buildings, and by regulations, which include altitude limits, minimum distance to people, and no-fly zones to name a few. Existing schemes for UAV path planning typically handle these constraints via shortest-path algorithms. However, in the context of aerial relays, the large number of degrees of freedom renders such an approach unaffordable. To bypass this difficulty, this work develops a framework built upon the notion of probabilistic roadmaps that allows the optimization of different communication performance metrics while preserving connectivity between the relays and the base station throughout the trajectory. To counteract the large number of configuration points required by conventional probabilistic roadmaps, a novel node generation scheme is developed based on two heuristics with theoretical guarantees, one for static users and another for moving users. Numerical experiments demonstrate that the proposed scheme can effectively serve the user by means of just two aerial relays.

Index Terms—Aerial relays, path planning, probabilistic roadmaps, aerial communications.

I. INTRODUCTION

Extending the coverage of cellular communication networks beyond cell limits is one of the many applications of autonomous unmanned aerial vehicles (UAVs) [1]. This need arises e.g. when terrestrial infrastructure is absent, as occurs in remote areas, or damaged by a natural disaster or military attack. Depending on the communication layers that they implement, UAVs that serve this purpose are referred to either as *aerial base stations* or as *aerial relays* [1].

This application has spurred a great amount of research in the last few years. For example, some works address the problem of placing aerial base stations at suitable locations to serve a collection of users on the ground that either remain static (see [2] and the references therein) or move (see e.g. [3], [4]). When it comes to aerial relays, many works focus on using a single UAV. Some consider remote regions with free space propagation (see e.g. [5]–[11]) whereas others can accommodate more complex scenarios such as urban environments (see e.g. [12]–[14]). However, long distances and obstructions call for multiple relays.

Some works considering multiple UAVs target the dissemination or collection of delay-tolerant information. There, the

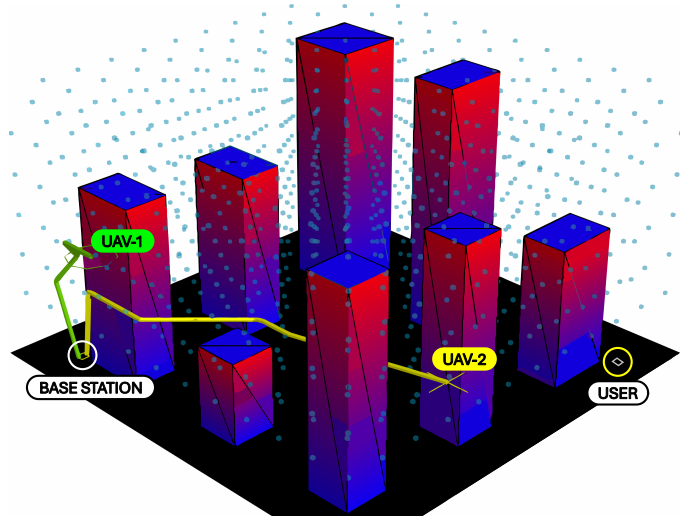


Fig. 1: Trajectories of two relay UAVs obtained with the proposed algorithm. Red/blue boxes represent buildings. The flight grid points are represented as blue dots. The green line is the trajectory of UAV-1, whose final position is at the green circle. The yellow line represents the trajectory of UAV-2, whose final position is the yellow cross.

UAVs deliver the data that they store on board by flying to the vicinity of its intended recipient (see e.g. [15], [16]) and, therefore, strictly speaking they may not be regarded as relays. Other works do consider multiple aerial relays that establish a *real-time* communication link between the user and the terrestrial base station (BS). The most common approaches in this context plan the paths of the UAVs via non-linear optimization over continuous variables, which comprise the spatial coordinates of all UAVs; see e.g. [17]–[23]. Unfortunately, these problems are non-convex, the solvers entail high complexity, and it is not generally possible to accommodate flight constraints. Other schemes, e.g. those based on mixed integer linear programs [24], [25] and the Steiner tree problem [26] also suffer from similar limitations.

In practice UAVs must accommodate the flight constraints imposed by regulations (e.g. no-flying zones, maximum and minimum heights, minimum distance to crowds, and so on) and by obstacles such as buildings. For this reason, most approaches for UAV path planning outside the aerial relay literature discretize the airspace and apply a shortest-path algorithm on the resulting graph [27]. Approaches of this kind

have been pursued for UAV communications e.g. to plan a path through coverage areas [28], but not to plan the trajectories of multiple aerial relays. The reason is that the degrees of freedom scale exponentially with the number of relays, which renders shortest-path algorithms computationally prohibitive.

The main novelty in this work is a framework for path planning of multiple aerial relays that can accommodate flight constraints. To sidestep the computational complexity of conventional shortest-path algorithms, the main idea is to build upon the *probabilistic roadmap* (PR) algorithm [29], where a shortest-path primitive is applied on a graph whose nodes are randomly generated. However, since the number of nodes required by conventional PR to ensure connectivity between the BS and the relays is prohibitively large, this algorithm is modified to draw the nodes around a tentative path that is judiciously designed by relying on a heuristic. It is worth noting that there have been works where PR has been applied to UAV path planning (see e.g. [30] and references therein) but, to the best of our knowledge, never for communications.

The main contributions of this work are

- C1 A general framework for planning the 3D path of multiple aerial relays such that (i) the relays maintain connectivity among themselves and with a terrestrial BS throughout their trajectories and (ii) the trajectory satisfies any given constraint on the flight region. The idea is to improve upon conventional PR by drawing the nodes of the graph around a heuristic waypoint sequence, which drastically reduces computational complexity and increases the optimality of the resulting path.
- C2 This approach is applied to devise an algorithm that approximately minimizes the time it takes to establish connectivity with a static remote user. The heuristic waypoint sequence designed for this scenario is theoretically guaranteed to connect the user to the BS using just two relays and is optimal in certain cases. An example of the trajectories of two relays obtained with this algorithm in an urban environment is illustrated in Fig. 1.
- C3 The approach in C1 is also applied to design another algorithm that either approximately minimizes the outage time or approximately maximizes the amount of transferred data when the user moves. The heuristic waypoint sequence utilized in this scenario enjoys similar theoretical guarantees to those in C2.
- C4 An extensive set of numerical experiments corroborates the effectiveness of the proposed algorithms in terms of multiple communication metrics.

After presenting the model and formulating the problem in Sec. II, PR is reviewed in Sec. III. Next, the proposed path planning algorithms are introduced in Sec. IV for a static user and in Sec. V for a moving user. Numerical experiments and conclusions are respectively presented in Secs. VI and VII. The developed simulator, the simulation code, and some videos can be found at https://github.com/uiano/pr_for_relay_path_planning.

Notation: Sets are notated by uppercase caligraphic letters. $|\mathcal{S}|$ is the cardinality of set \mathcal{S} . $\mathcal{A} \times \mathcal{B} \triangleq \{(a, b) : a \in \mathcal{A}, b \in \mathcal{B}\}$ is the Cartesian product of sets \mathcal{A} and \mathcal{B} , where (a, b) denotes a tuple. \mathbb{R}_+ is the set of non-negative real numbers. Boldface up-

percase (lowercase) letters denote matrices (column vectors). $\|\mathbf{q}\|$ stands for the ℓ_2 -norm of vector \mathbf{q} . $\mathcal{I}[\cdot]$ is a function that returns 1 if the condition inside is true and 0 otherwise. $\min(a, b)$ and $\max(a, b)$ respectively denote the minimum and maximum between a and b . $\dot{\mathbf{q}}(t)$ stands for the entrywise first derivative of $\mathbf{q}(t)$ with respect to t . $\lfloor a \rfloor$ is the largest integer that is less than or equal to a .

II. THE PATH PLANNING PROBLEM

This section presents the model and problem formulation.

A. Model

Consider a spatial region $\mathcal{S} \subset \mathbb{R}^3$ and let $\mathcal{F} \subset \mathcal{S}$ denote the set of points above the ground and outside any building or obstacle. For simplicity, it is assumed that $[x, y, z]^\top \in \mathcal{F}$ implies $[x, y, z']^\top \in \mathcal{F}$ for all $z' \geq z$, which essentially means that the buildings or obstacles contain no holes or parts that stand out. To establish a link between a base station (BS) at location $\mathbf{q}_{\text{BS}} \triangleq [x_{\text{BS}}, y_{\text{BS}}, z_{\text{BS}}]^\top \in \mathcal{S}$ and the user equipment (UE) with trajectory¹ $\{\mathbf{q}_{\text{UE}}(t) \triangleq [x_{\text{UE}}(t), y_{\text{UE}}(t), z_{\text{UE}}(t)]^\top, t \geq 0\} \subset \mathcal{S}$, a total of K aerial relays are deployed. Let $\bar{\mathcal{F}} \subset \mathcal{F}$ be the set of spatial locations where the UAVs can fly. This can be determined by regulations (e.g. the minimum and maximum allowed altitudes, no-fly zones, and so on) or any other operational constraints. The position of the k -th UAV at time t is represented as $\mathbf{q}_k(t) \in \bar{\mathcal{F}}$ and the positions of all UAVs at time t are collected into the $3 \times K$ matrix $\mathbf{Q}(t) \triangleq [\mathbf{q}_1(t), \dots, \mathbf{q}_K(t)]$, referred to as the *configuration point* (CP) at time t [29]. The set of all matrices whose columns are in $\bar{\mathcal{F}}$ is the so-called *configuration space* (\mathcal{Q} -space) and will be denoted as \mathcal{Q} . The UAVs collectively follow a trajectory $\mathcal{T} \triangleq \{\mathbf{Q}(t), t \geq 0\} \subset \mathcal{Q}$. The take-off locations of the UAVs are collected in matrix $\mathbf{Q}_0 \triangleq \mathbf{Q}(0)$ and the maximum speed is v_{max} .

The targeted link must convey information in both ways but, to simplify the exposition, the focus here will be on the downlink. There, the signal transmitted by the BS is first decoded and retransmitted by UAV-1. The signal transmitted by UAV-1 is decoded and retransmitted by UAV-2 and so on, until the UE receives the signal retransmitted by UAV- K . Relays employ capacity-attaining codes and the interference between hops is ignored.

Besides the data to be relayed towards the UE, each UAV consumes a rate r_{CC} for command and control. This means that the achievable rate between the BS and UAV- k for a generic CP $\mathbf{Q} \triangleq [\mathbf{q}_1, \dots, \mathbf{q}_K]$ can be recursively obtained as

$$r_k(\mathbf{Q}) = \max(0, \min(r_{k-1}(\mathbf{Q}) - r_{\text{CC}}, c(\mathbf{q}_{k-1}, \mathbf{q}_k))), \quad (1)$$

where $c(\mathbf{q}, \mathbf{q}')$ denotes the channel capacity between a UAV at \mathbf{q} and a UAV at \mathbf{q}' and $r_1(\mathbf{Q}) = c(\mathbf{q}_{\text{BS}}, \mathbf{q}_1)$. Similarly, the achievable rate of the UE when it is at \mathbf{q}_{UE} is

$$r_{\text{UE}}(\mathbf{Q}, \mathbf{q}_{\text{UE}}) = \max(0, \min(r_K(\mathbf{Q}) - r_{\text{CC}}, c(\mathbf{q}_K, \mathbf{q}_{\text{UE}}))). \quad (2)$$

¹Formally, a trajectory is a function. However, set notation is adopted throughout for concision.

The second argument in r_{UE} will be omitted when it is clear from the context. Throughout the trajectory, the UAVs must have connectivity with the BS, which means that $r_k(\mathbf{Q}(t)) \geq r_{\text{CC}} \forall k, t$. Meanwhile, the UE is said to have connectivity with the BS if $r_{\text{UE}}(\mathbf{Q})$ exceeds a given target rate r_{UE}^{\min} .

To plan the trajectory, it is necessary to know function $c(\mathbf{q}, \mathbf{q}')$. In practice, one needs to resort to some approximation. For example, one can use a channel-gain map [31], a 3D terrain/city model together with a ray-tracing algorithm, a line-of-sight (LOS) map [32], a set of bounding boxes known to contain the buildings and other obstacles, specific models for UAV channels, and so on. As an example, a LOS map $c(\mathbf{q}, \mathbf{q}')$ is a decreasing function $c(d)$ of the distance $d = \|\mathbf{q} - \mathbf{q}'\|$ whenever there is LOS between \mathbf{q} and \mathbf{q}' and 0 otherwise. For example, if B is the bandwidth and the noise power spectral density is 1 without loss of generality, $c(d)$ can be given by

$$c(d) = B \log_2 \left(1 + P_t G_t G_r \left(\frac{\lambda}{4\pi d} \right)^2 \right), \quad (3)$$

where P_t , G_t , G_r , and λ are respectively the transmit power, transmit gain, receive gain, and wavelength. Although $c(0)$ is not defined, to simplify some expressions it is useful to assume that it is a very large constant. LOS maps are suitable to high-frequency communications, such as mmWave, where the absorption introduced by obstacles is large [2].

B. Problem Formulation

This paper addresses the problem of designing the trajectory for the UAVs to establish connectivity between the UE and the BS. Given \mathbf{q}_{BS} , $\mathbf{Q}_0 \in \mathcal{Q}$, $\mathbf{q}_{\text{UE}}(t)$, K , c , r_{CC} , r_{UE}^{\min} , and v_{max} , the problem is to solve

$$\underset{\mathcal{T}}{\text{minimize}} \quad J(\mathcal{T}) \quad (4a)$$

$$\text{s.t.} \quad \mathbf{Q}(t) \in \mathcal{Q} \quad \forall t, \quad \mathbf{Q}(0) = \mathbf{Q}_0 \quad (4b)$$

$$r_k(\mathbf{Q}(t)) \geq r_{\text{CC}} \quad \forall k, t \quad (4c)$$

$$\|\dot{\mathbf{q}}_k(t)\| \leq v_{\text{max}} \quad \forall k, t, \quad (4d)$$

where $J(\mathcal{T})$ is the objective function. Several possibilities are discussed next:

- **Connection time.** In many situations, it is desirable to establish connectivity between the UE and the BS as soon as possible. This is the case when time-sensitive information must be delivered in a short time, e.g. to notify a user of a tsunami, earthquake, or military attack. The goal is therefore to minimize the *connection time*

$$J(\mathcal{T}) = T_c(\mathcal{T}) \triangleq \inf\{t : r_{\text{UE}}(\mathbf{Q}(t), \mathbf{q}_{\text{UE}}(t)) \geq r_{\text{UE}}^{\min}\}. \quad (5)$$

Note that, consistent with the standard convention for the infimum, $T_c(\mathcal{T}) = \infty$ if $r_{\text{UE}}(\mathbf{Q}(t), \mathbf{q}_{\text{UE}}(t)) \geq r_{\text{UE}}^{\min}$ does not hold for any t .

Note that a low $J(\mathcal{T})$ may not be meaningful if the UE loses connectivity right after the connection is established, which can happen if the UE moves. This renders the connection time immaterial unless the UE is static.

- **Outage time.** A natural objective when the UE is not static is the time during which it has no connectivity [33]. This leads to minimizing the *outage time*

$$J(\mathcal{T}) = \int_0^T \mathcal{I}[r_{\text{UE}}(\mathbf{Q}(t), \mathbf{q}_{\text{UE}}(t)) < r_{\text{UE}}^{\min}] dt, \quad (6)$$

where T is a given time horizon and $\mathcal{I}[\cdot]$ was defined in Sec. I.

- **Transferred data.** In some applications, data may be relatively delay tolerant. Thus, instead of minimizing outage time, one may be interested in maximizing the total amount of data received by the UE within a given time horizon T . This gives rise to the objective function

$$J(\mathcal{T}) = - \int_0^T r_{\text{UE}}(\mathbf{Q}(t), \mathbf{q}_{\text{UE}}(t)) dt, \quad (7)$$

where the minus sign is due to the fact that (4) is a minimization problem.

Finally, note that (4) does not enforce a minimum distance between UAVs for simplicity. However, such a constraint can be readily accommodated in the proposed scheme.

III. PATH PLANNING VIA PROBABILISTIC ROADMAPS

Since Problem (4) involves the optimization with respect to a trajectory, which comprises infinitely many CPs, the exact solution cannot generally be found by numerical means. Instead, as customary in UAV path planning, both spatial and temporal discretizations will be introduced.

Specifically, the flight region $\bar{\mathcal{F}}$ is discretized into a regular 3D *flight grid* $\bar{\mathcal{F}}_G \subset \bar{\mathcal{F}} \subset \mathbb{R}^3$, whose points are separated along the x, y, and z axes respectively by δ_x , δ_y , and δ_z ; see Fig. 1. To simplify some expressions, it will be assumed that the take-off locations of the UAVs are in $\bar{\mathcal{F}}_G$. This spatial discretization also induces a grid \mathcal{Q}_G in the Q-space, which e.g. for $K = 2$ is given by $\mathcal{Q}_G \triangleq \bar{\mathcal{F}}_G \times \bar{\mathcal{F}}_G$.

Regarding the time-domain discretization, the trajectory \mathcal{T} will be designed by first finding a CP sequence $P \triangleq \{\mathbf{Q}[0], \dots, \mathbf{Q}[N-1]\}$ through the grid \mathcal{Q}_G . This sequence will be referred to as *combined path*, whereas the sequence of waypoints $\mathbf{q}_k[n]$ that each individual UAV must follow will be referred to as a *path*. Given P , the trajectory \mathcal{T} is recovered by interpolating the waypoints in P . A path P will be said to be feasible iff the associated trajectory \mathcal{T} is feasible.

Having introduced the discretization, the next step is to discuss approaches to obtain a feasible waypoint sequence that attains a satisfactory objective value. Conventional algorithms for planning the path of a single UAV create a graph whose nodes are the points of $\bar{\mathcal{F}}_G$ and where an edge exists between two nodes if the associated points are adjacent on the grid. In a 3D regular grid like $\bar{\mathcal{F}}_G$, each point has typically 26 adjacent points, which renders the application of shortest-path algorithms on such a graph viable. However, the grid \mathcal{Q}_G has exponentially many more points than $\bar{\mathcal{F}}_G$. For example, if $\bar{\mathcal{F}}_G$ is a (small) $10 \times 10 \times 10$ grid, then \mathcal{Q}_G has 10^{3K} points. Besides, since each of them has generally $27^K - 1$ adjacent points, solving (4) via shortest-path algorithms is prohibitive.

To bypass this kind of difficulties, the seminal paper [29] proposed the PR algorithm, which consists of 3 steps: Step 1: a

node set $\mathcal{N} \subset \mathcal{Q}$ with a much smaller number of nodes than \mathcal{Q}_G is randomly generated at random. Step 2: the edge set $\mathcal{E} \subset \mathcal{N} \times \mathcal{N}$ is constructed by connecting the nodes corresponding to CPs \mathbf{Q} and \mathbf{Q}' if they are nearest neighbors and it is possible to transition directly from \mathbf{Q} to \mathbf{Q}' . Step 3: a shortest path is found on the graph with node set \mathcal{N} and edge set \mathcal{E} .

Unfortunately, the complexity reduction of PR comes at a cost: the number of nodes in \mathcal{N} necessary to find a feasible (let alone satisfactory) path may be very large. The key idea in this paper is to solve (4) by modifying PR to counteract the aforementioned limitation: the node generation (sampling) in Step 1 is carried out in such a way that Step 3 can always find a feasible waypoint sequence that attains a satisfactory objective. The idea, described in the following sections, relies on a heuristic to obtain an initial combined path.

IV. PATH PLANNING FOR STATIC UE

Although the scenario where the UE is static is a special case of the general problem obtained by setting $\mathbf{q}_{UE}(t) = \mathbf{q}_{UE}$ for all t , it is convenient to address the static case separately since it affords a simpler algorithm with lower complexity and facilitates the exposition. To this end, this section applies the approach described in Sec. III — the case of a moving UE will be addressed in Sec. V. Specifically, Sec. IV-B adapts PR to solve (4) when $\mathbf{q}_{UE}(t) = \mathbf{q}_{UE} \forall t$ by relying on the tentative path produced by the technique proposed in Sec. IV-A. Due to the reasons in Sec. II-B, the objective in (5) will be adopted.

A. Planning the Tentative Path

A combined path P is said to be *valid* if it is feasible and attains a finite connection time $T_c(\mathcal{T})$. Equivalently, $P \triangleq \{\mathbf{Q}[0], \dots, \mathbf{Q}[N-1]\}$ is valid if it is feasible and $\exists n : r_{UE}(\mathbf{Q}[n]) \geq r_{UE}^{\min}$. A feasible path P on a grid \mathcal{Q}_G is said to be *optimal* if it attains the lowest connection time among all feasible paths on \mathcal{Q}_G . This section proposes a heuristic that is guaranteed to find a valid path under general conditions. In some situations, this path will even be optimal.

While the general approach in this paper is applicable to an arbitrary K , the heuristics developed here are specialized to the case $K = 2$. To motivate this assumption, the first result establishes that 2 UAVs suffice to guarantee the existence of a valid path under general conditions.

Proposition 1: Let h denote the height of the highest obstacle and suppose that the UAVs can fly above h . Let c be a LOS map. Furthermore, let $d \triangleq \sqrt{(x_{UE} - x_{BS})^2 + (y_{UE} - y_{BS})^2}$ denote the horizontal distance between the BS and the UE and assume that $\mathbf{q}_k(0) = \mathbf{q}_{BS} \forall k$. If $h < \min(z_{UE} + c^{-1}(r_{UE}^{\min}), z_{BS} + c^{-1}(r_{UE}^{\min} + 2r_{CC}))$ and $d \leq c^{-1}(r_{UE}^{\min} + r_{CC})$, there exists a valid trajectory \mathcal{T} with $K = 2$ for Problem (4).

Proof: Let $z = \min(z_{UE} + c^{-1}(r_{UE}^{\min}), z_{BS} + c^{-1}(r_{UE}^{\min} + 2r_{CC}))$ and suppose that $K = 2$. It is easy to show that if UAV-1 navigates to $\mathbf{q}_1 \triangleq [x_{BS}, y_{BS}, z]^T$ and UAV-2 navigates first to \mathbf{q}_1 and later to $\mathbf{q}_2 \triangleq [x_{UE}, y_{UE}, z]^T$, then \mathcal{T} is feasible and $T_c(\mathcal{T}) < (z - z_{BS} + d)/v_{\max}$. ■

Thus, so long as d and h are not too large relative to r_{UE}^{\min} and r_{CC} , a valid trajectory exists with only 2 relays. For this reason, the rest of this section focuses on the case $K = 2$.

Note that the proof of Proposition 1 also provides a valid path. However, to apply PR it is preferable to adopt the approach in this section since it yields a path that is also valid and, in addition, attains a significantly smaller objective; cf. Sec. VI. The idea is to first generate the path for UAV-2. Then, a path is found for UAV-1 to serve UAV-2 throughout. If this is not possible, the path of UAV-2 is *lifted* until it becomes possible.

Before delving into the procedure, some notation and terminology needs to be introduced. Upon letting $\mathcal{R}(\mathbf{q}, r) \triangleq \{\mathbf{q}' \in \bar{\mathcal{F}}_G : c(\mathbf{q}, \mathbf{q}') \geq r\}$, it is clearly necessary (but not sufficient) that UAV-1 is in $\mathcal{R}(\mathbf{q}_{BS}, 2r_{CC})$ throughout the path and in $\mathcal{R}(\mathbf{q}_{BS}, 2r_{CC} + r_{UE}^{\min})$ at the moment of establishing connectivity with the UE. Similarly, with notation $\mathcal{R}(\mathbf{q}, r, r') \triangleq \{\mathbf{q}'' \in \bar{\mathcal{F}}_G | \exists \mathbf{q}' \in \mathcal{R}(\mathbf{q}, r) : c(\mathbf{q}', \mathbf{q}'') \geq r'\}$, it is necessary (not sufficient) that UAV-2 is in $\mathcal{N}_2 \triangleq \mathcal{R}(\mathbf{q}_{BS}, 2r_{CC}, r_{CC})$ throughout the path and in $\mathcal{D}_2 \triangleq \mathcal{R}(\mathbf{q}_{BS}, 2r_{CC} + r_{UE}^{\min}, r_{CC} + r_{UE}^{\min}) \cap \mathcal{R}(\mathbf{q}_{UE}, r_{UE}^{\min})$ at the moment of establishing connectivity with the UE. For simplicity, a grid point \mathbf{q}_2 will be referred to as a *candidate* location of UAV-2 if $\mathbf{q}_2 \in \mathcal{N}_2$, whereas \mathbf{q}_2 will be named a *destination* of UAV-2 if $\mathbf{q}_2 \in \mathcal{D}_2$. Throughout the paper, the term *candidate* will refer to a set of points where a UAV is *required* to be because otherwise the UAVs will not meet the r_{CC} requirement. The term *destination* will refer to a set of locations where the UAV is *desired* to be since there the UE may receive r_{UE}^{\min} .

1) *Path for UAV-2:* The idea is to start by first planning the path of UAV-2 by finding the shortest path (e.g. via Dijkstra's algorithm) from the given $\mathbf{q}_2[0] = \mathbf{q}_2(0)$ to the nearest point in $\mathcal{D}_2 \subset \mathcal{N}_2$ through a graph with node set \mathcal{N}_2 . In this graph, two nodes \mathbf{q} and \mathbf{q}' are connected if they are adjacent in $\bar{\mathcal{F}}_G$, which will be denoted as $(\mathbf{q}, \mathbf{q}') \in \mathcal{E}_{\bar{\mathcal{F}}_G}$. Since the objective in (4) is the connection time, the weight of an edge $(\mathbf{q}, \mathbf{q}')$ can be set to $\|\mathbf{q} - \mathbf{q}'\|$ since this distance is proportional to the time it takes for UAV-2 to travel from \mathbf{q} to \mathbf{q}' at full speed v_{\max} .

This procedure produces a path $\{\mathbf{q}_2[0], \mathbf{q}_2[1], \dots, \mathbf{q}_2[N_0 - 1]\}$, where N_0 is the length of the shortest path. The algorithm is summarized as Algorithm 1.

2) *Path for UAV-1:* If there exists a path for UAV-1 through $\bar{\mathcal{F}}_G$ that provides a sufficient rate to UAV-2 at all the waypoints $\mathbf{q}_2[0], \mathbf{q}_2[1], \dots, \mathbf{q}_2[N_0 - 1]$, the combined path will not only be valid but also optimal. As seen later, this will often be the case, but not always. Formally, for the combined path to be feasible, the position of UAV-1 must satisfy $\mathbf{q}_1 \in \mathcal{N}_1[n] \triangleq \mathcal{R}(\mathbf{q}_{BS}, 2r_{CC}) \cap \mathcal{R}(\mathbf{q}_2[n], r_{CC})$ when UAV-2 is at $\mathbf{q}_2[n]$. Besides, for the path to be valid, it is required that $\mathbf{q}_1 \in \mathcal{D}_1 \triangleq \mathcal{R}(\mathbf{q}_{BS}, 2r_{CC} + r_{UE}^{\min}) \cap \mathcal{R}(\mathbf{q}_2[N_0 - 1], r_{CC} + r_{UE}^{\min}) \subset \mathcal{N}_1[N_0 - 1]$ once UAV-2 reaches $\mathbf{q}_2[N_0 - 1]$. In terms of the terminology introduced earlier, \mathbf{q}_1 is a *candidate* location at time step n if $\mathbf{q}_1 \in \mathcal{N}_1[n]$ and a *destination* if $\mathbf{q}_1 \in \mathcal{D}_1$.

Since the set of candidate positions depends on n , the path must be planned through an *extended graph*. Upon letting the set of extended nodes at time n be $\bar{\mathcal{N}}_1[n] \triangleq \{(n, \mathbf{q}) \mid \mathbf{q} \in \mathcal{N}_1[n]\}$, the node set of this graph is $\bar{\mathcal{N}}_1 \triangleq \cup_n \bar{\mathcal{N}}_1[n]$. Initially, one can think of finding a path $(0, \mathbf{q}_1[0]), (1, \mathbf{q}_1[1]), \dots, (N_0 - 1, \mathbf{q}_1[N_0 - 1])$ such that $(n, \mathbf{q}_1[n]) \in \bar{\mathcal{N}}_1[n] \forall n, \mathbf{q}_1[N_0 - 1] \in \mathcal{D}_1$, and $(\mathbf{q}_1[n], \mathbf{q}_1[n+1]) \in \mathcal{E}_{\bar{\mathcal{F}}_G} \forall n$. If this is possible, then the combined path $\{\mathbf{Q}[n] = [\mathbf{q}_1[n], \mathbf{q}_2[n]], n = 0, \dots, N_0 - 1\}$, is, as indicated earlier, optimal. For the cases where it is

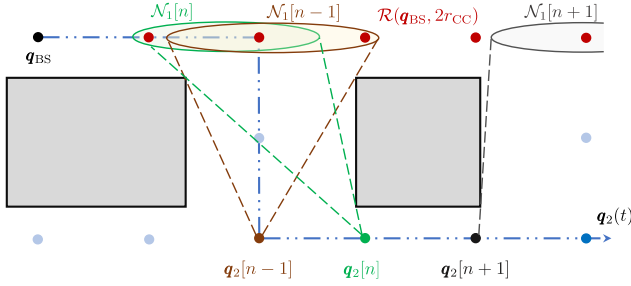


Fig. 2: Top view of an example case where no path through adjacent points exists that allows UAV-1 to serve UAV-2 throughout the path of the latter. At some point, UAV-2 may need to wait so that UAV-1 can gain altitude. Grey boxes represent buildings and dots are grid points.

not possible, two techniques are presented: *waiting* and *lifting*.

Waiting. The aforementioned optimal combined path can certainly be found when UAV-1 can maintain the connectivity of UAV-2 just by moving to adjacent locations on $\bar{\mathcal{F}}_G$. However, this may not be the case: sometimes UAV-1 may need to perform multiple steps through adjacent locations on $\bar{\mathcal{F}}_G$ to fly around obstacles in order to guarantee the connectivity of UAV-2; see Fig. 2. In other words, UAV-2 may need to wait at a certain waypoint until UAV-1 adopts a suitable location. To allow for this possibility, the form of the path of UAV-1 is generalized to be $(n_0, \mathbf{q}_1[0]), (n_1, \mathbf{q}_1[1]), \dots, (n_{\tilde{N}-1}, \mathbf{q}_1[\tilde{N}-1])$ for some \tilde{N} , where $(n_i, \mathbf{q}_1[i]) \in \tilde{\mathcal{N}}_1[n_i]$, $n_0 = 0$, $\mathbf{q}_1[\tilde{N}-1] \in \mathcal{D}_1$, $n_{i-1} \leq n_i \leq n_{i-1} + 1$, and $(\mathbf{q}_1[i], \mathbf{q}_1[i+1]) \in \mathcal{E}_{\bar{\mathcal{F}}_G}$ for all i . In words, the index n_i need not increase monotonically, it suffices that it does not decrease. The corresponding sequence of waypoints for UAV-2 will be $\mathbf{q}_2[n_0], \mathbf{q}_2[n_1], \dots, \mathbf{q}_2[n_{\tilde{N}-1}]$. This means that UAV-2 *waits* at $\mathbf{q}_2[n_i]$ whenever $n_i = n_{i+1}$.

To accommodate this possibility, nodes (n, \mathbf{q}) and (n', \mathbf{q}') must be connected iff $(\mathbf{q}, \mathbf{q}') \in \mathcal{E}_{\bar{\mathcal{F}}_G}$ and $n \leq n' \leq n+1$. The weight of an edge between (n, \mathbf{q}) and (n', \mathbf{q}') is $\|\mathbf{q} - \mathbf{q}'\|$.

Lifting. In certain cases, a path for UAV-1 may not be found even with the waiting technique. To remedy this, one can *lift* the path of UAV-2 to expand the set of candidate locations of UAV-1. To this end, let h_{\max} be the height of the lowest level in $\bar{\mathcal{F}}_G$ that is higher than all obstacles. Also, for $\mathbf{q} \in \bar{\mathcal{F}}_G$, let

$$L(\mathbf{q}) \triangleq \begin{cases} \mathbf{q} + [0, 0, \delta_z]^\top & \text{if } [0, 0, 1]\mathbf{q} + \delta_z \leq h_{\max}, \\ \mathbf{q} & \text{otherwise,} \end{cases} \quad (8)$$

where δ_z is the spacing along the z-axis between two consecutive levels in $\bar{\mathcal{F}}_G$ and the inner product $[0, 0, 1]\mathbf{q}$ returns the z-component (altitude) of \mathbf{q} . Additionally, it is convenient to recursively let $L^{(i)}(\mathbf{q}) \triangleq L(L^{(i-1)}(\mathbf{q}))$, where $L^{(1)}(\mathbf{q}) \triangleq L(\mathbf{q})$.

To extend operator L to paths, let $p_2 \triangleq \{\mathbf{q}_2[0], \mathbf{q}_2[1], \dots, \mathbf{q}_2[N_0-1]\}$ be the path of UAV-2 provided by Algorithm 1. Also, let $u_{\max}^\uparrow \triangleq \min\{u : L^{(u)}(\mathbf{q}_2[0]) = L^{(u+1)}(\mathbf{q}_2[0])\}$ and $u_{\max}^\downarrow \triangleq \min\{u : L^{(u)}(\mathbf{q}_2[N_0-1]) = L^{(u+1)}(\mathbf{q}_2[N_0-1])\}$ respectively denote the maximum number of times that the initial and final points of p_2 can be lifted. The operator $L^{(u)}(p_2)$ returns the path that results from concatenating the following paths:

- 1) an ascent path $\{\mathbf{q}_2[0], L^{(1)}(\mathbf{q}_2[0]), \dots, L^{(u^\uparrow-1)}(\mathbf{q}_2[0])\}$, where $u^\uparrow \triangleq \min(u, u_{\max}^\uparrow)$,
- 2) the shortest path $\{\mathbf{q}_2^{(u)}[0], \dots, \mathbf{q}_2^{(u)}[N_u-1]\}$ from $\mathbf{q}_2^{(u)}[0] \triangleq L^{(u^\uparrow)}(\mathbf{q}_2[0])$ to $\mathbf{q}_2^{(u)}[N_u-1] \triangleq L^{(u^\downarrow)}(\mathbf{q}_2[N_0-1])$ in the graph of Sec. IV-A1, where $u^\downarrow \triangleq \min(u, u_{\max}^\downarrow)$, and
- 3) the descent path $\{L^{(u^\downarrow-1)}(\mathbf{q}_2[N_0-1]), L^{(u^\downarrow-2)}(\mathbf{q}_2[N_0-1]), \dots, \mathbf{q}_2[N_0-1]\}$.

Lifting the path of UAV-2 expands the set of candidate locations for UAV-1. This motivates iteratively lifting the path of UAV-2 until a suitable path for UAV-1 can be found. Such a procedure is summarized in Algorithm 2.

3) *Theoretical Guarantees:* The procedure described above and summarized in Algorithm 2 is guaranteed to eventually succeed under broad conditions:

Theorem 1: Let $\bar{\mathcal{F}}_G$ be a sufficiently dense regular grid and let $\mathbf{Q}[0] = [\mathbf{q}_{BS}, \mathbf{q}_{BS}]$. With the LOS map model introduced in Sec. II-A, suppose that $r_{UE}^{\min} \geq 4r_{CC}$ and $h_{\max} \leq \sqrt{[c^{-1}(2r_{CC})]^2 - [c^{-1}(2r_{CC} + r_{UE}^{\min})]^2}$. If a valid path for (4) when $J(\mathcal{T}) = T_c(\mathcal{T})$ exists through waypoints in \mathcal{Q}_G , then the tentative path $P^V \triangleq \{\mathbf{q}_1[i], \hat{\mathbf{q}}_2[n_i], i = 0, \dots, \tilde{N}-1\}$ obtained from Algorithm 2 is valid. In addition, if no lifting steps are used and $\hat{\mathbf{q}}_2[n_i] \neq \hat{\mathbf{q}}_2[n_{i+1}] \forall i$, then P^V is optimal.

Proof: See Appendix A. \blacksquare

Thus, if r_{UE}^{\min} and r_{CC} are not too large relative to the size of the region, the approach in this section results in a valid combined path whenever such a path exists.

B. Probabilistic Roadmaps with Feasible Initialization

This section adapts PR to solve (4) by relying on the tentative path produced by Algorithm 2.

1) *Construction of the Node Set:* As described earlier, the first step in PR is to randomly generate a set \mathcal{N} of CPs. The sampled distribution drastically impacts the optimality of the resulting combined path and the computational burden of the algorithm. In the work at hand, \mathcal{N} will comprise all the CPs of the path $P^V = \{\mathbf{Q}[0], \dots, \mathbf{Q}[\tilde{N}-1]\}$ from Sec. IV-A together with C additional CPs drawn at random around the CPs in P^V .

Specifically, for each $\mathbf{Q} = [\mathbf{q}_1, \mathbf{q}_2] \in P^V$, the proposed sampling strategy generates $\lfloor C/\tilde{N} \rfloor$ configuration points $\tilde{\mathbf{Q}} = [\tilde{\mathbf{q}}_1, \tilde{\mathbf{q}}_2]$ as follows. First, generate $\tilde{\mathbf{q}}_1$ by drawing a point of $\mathcal{R}(\mathbf{q}_{BS}, 2r_{CC}) - \{\mathbf{q}_1\}$ with probability proportional to $1/\|\tilde{\mathbf{q}}_1 - \mathbf{q}_1\|$. Next, independently of $\tilde{\mathbf{q}}_1$, generate $\tilde{\mathbf{q}}_2$ by drawing a point of $\mathcal{R}(\mathbf{q}_{BS}, 2r_{CC}, r_{CC}) - \{\mathbf{q}_2\}$ with probability proportional to $1/\|\tilde{\mathbf{q}}_2 - \mathbf{q}_2\|$. If $\tilde{\mathbf{q}}_2 \notin \mathcal{R}(\tilde{\mathbf{q}}_1, r_{CC})$, another pair $(\tilde{\mathbf{q}}_1, \tilde{\mathbf{q}}_2)$ is generated until $\tilde{\mathbf{q}}_2 \in \mathcal{R}(\tilde{\mathbf{q}}_1, r_{CC})$, which will eventually happen as $\tilde{\mathbf{q}}_2 \in \mathcal{R}(\mathbf{q}_{BS}, 2r_{CC}, r_{CC})$.

This procedure, which is based on the distance to CPs in P^V , ensures that many of the sampled CPs lie close to the tentative path while others may be farther away, thereby increasing the chances for finding near-optimal paths.

2) *Construction of the Edge Set:* The next step is to construct the edge set of a nearest neighbor graph whose node set was generated in Sec. IV-B1. To obtain trajectories with a lower connection time, it is convenient not to require that each UAV moves through adjacent points in $\bar{\mathcal{F}}_G$: what matters is that the UAVs can move from one CP to another (i) without losing connectivity and (ii) without abandoning $\bar{\mathcal{F}}$.

Algorithm 1: Tentative Path UAV-2, Static UE

input: $\bar{\mathcal{F}}_G, \mathbf{q}_{BS}, \mathbf{q}_{UE}, r_{CC}, r_{UE}^{\min}, \mathbf{q}_2[0]$

- 1: Find candidate locations of UAV-2
 $\rightarrow \mathcal{N}_2 = \mathcal{R}(\mathbf{q}_{BS}, 2r_{CC}, r_{CC})$
- 2: Find destinations of UAV-2
 $\rightarrow \mathcal{D}_2 = \mathcal{R}(\mathbf{q}_{BS}, 2r_{CC} + r_{UE}^{\min}, r_{CC} + r_{UE}^{\min}) \cap \mathcal{R}(\mathbf{q}_{UE}, r_{UE}^{\min})$
- 3: Construct graph \mathcal{G}_1 with weights $w(\mathbf{q}, \mathbf{q}') = \|\mathbf{q} - \mathbf{q}'\|$
- 4: **return** $p_2 := \text{shortest_path}(\mathbf{q}_2[0], \mathcal{D}_2)$

Thus, an edge $(\mathbf{Q}, \mathbf{Q}')$ is added to the edge set if \mathbf{Q} and \mathbf{Q}' are nearest neighbors and conditions (i) and (ii) are satisfied. To numerically check these conditions, one can verify that they hold for a finite set of points in the line segment between \mathbf{Q} and \mathbf{Q}' . Due to the considered objective function, the weight of an edge between $\mathbf{Q} = [\mathbf{q}_1, \mathbf{q}_2]$ and $\mathbf{Q}' = [\mathbf{q}'_1, \mathbf{q}'_2]$ will be given by the time that the UAVs require to move from \mathbf{Q} to \mathbf{Q}' . Given the speed constraint (4d), this time is determined by the UAV that traverses the longest distance and, therefore, equals $\max_k \|\mathbf{q}_k - \mathbf{q}'_k\|/v_{\max}$.

3) *Path Planning in Q-Space:* After the nearest-neighbor graph is constructed, a shortest path is sought from \mathbf{Q}_0 to any of the CPs $[\mathbf{q}_1, \mathbf{q}_2]$ that satisfy $\mathbf{q}_1 \in \mathcal{R}(\mathbf{q}_{BS}, 2r_{CC} + r_{UE}^{\min})$ and $\mathbf{q}_2 \in \mathcal{R}(\mathbf{q}_1, r_{CC} + r_{UE}^{\min}) \cap \mathcal{R}(\mathbf{q}_{UE}, r_{UE}^{\min})$. The resulting CP sequence P^{PR} will never have a greater objective than the tentative path P^V provided that all consecutive CPs in P^V are connected in the PR graph, which holds so long as $\bar{\mathcal{F}}_G$ is sufficiently dense.

C. From the Waypoint Sequence to the Trajectory

Given the waypoint sequence $P^{\text{PR}} = \{\mathbf{Q}[0], \dots, \mathbf{Q}[N^{\text{PR}} - 1]\}$ obtained in the previous step, it remains only to obtain the trajectory $\mathcal{T}^{\text{PR}} = \{\mathbf{Q}(t), t \geq 0\}$. To this end, it is necessary to determine the time at which the UAVs arrive at each of the waypoints $\mathbf{Q}[n]$. As indicated in Sec. IV-B3, the time it takes to arrive at $\mathbf{Q}[n] = [\mathbf{q}_1[n], \mathbf{q}_2[n]]$ from $\mathbf{Q}[n-1] = [\mathbf{q}_1[n-1], \mathbf{q}_2[n-1]]$ is $\max_k \|\mathbf{q}_k[n] - \mathbf{q}_k[n-1]\|/v_{\max}$. Let t_n represent the time at which the UAVs arrive at $\mathbf{Q}[n]$ and let $t_0 = 0$. In this case, it clearly holds that

$$t_n = t_{n-1} + \frac{\max_k \|\mathbf{q}_k[n] - \mathbf{q}_k[n-1]\|}{v_{\max}}. \quad (9)$$

This provides $\mathbf{Q}(t_n) = \mathbf{Q}[n]$ for $n = 0, \dots, N^{\text{PR}} - 1$. For $t \geq t_{N^{\text{PR}}-1}$, one can simply set $\mathbf{Q}(t) = \mathbf{Q}(t_{N^{\text{PR}}-1})$. The CPs $\mathbf{Q}(t)$ for other values of t will be determined by the flight controller, which may be provided just a sequence of waypoints along with their times. For simulation, one can use linear interpolation to resample $\mathbf{Q}(t)$ at uniform intervals.

The scheme is summarized as Algorithm 3 and will be referred to as *PR with feasible initialization* (PRFI) for static UE.

V. PATH PLANNING FOR MOVING UE

This section applies the approach in Sec. III to solve (4) when the UE moves. For the reasons provided in Sec. II-B, the focus will be on optimizing the outage time (6) and the amount of transferred data (7).

Algorithm 2: Tentative Path UAV-1, Static UE

input: $\bar{\mathcal{F}}_G, \mathbf{q}_{BS}, \mathbf{q}_{UE}, r_{CC}, r_{UE}^{\min}, \mathbf{q}_1[0], p_2$

- 1: **for** $u = 0, 1, \dots$ **do**
- 2: $\{\hat{\mathbf{q}}_2[0], \hat{\mathbf{q}}_2[1], \dots, \hat{\mathbf{q}}_2[N_u - 1]\} := L^{(u)}(p_2)$
- 3: Find candidate locations of UAV-1
 $\rightarrow \mathcal{N}_1[n] = \mathcal{R}(\mathbf{q}_{BS}, 2r_{CC}) \cap \mathcal{R}(\hat{\mathbf{q}}_2[n], r_{CC})$
- 4: Find destinations of UAV-1 $\rightarrow \mathcal{D}_1 = \mathcal{R}(\mathbf{q}_{BS}, 2r_{CC} + r_{UE}^{\min}) \cap \mathcal{R}(\hat{\mathbf{q}}_2[N_u - 1], r_{CC} + r_{UE}^{\min})$
- 5: Construct extended graph \mathcal{G}_2 with weights as in Sec. IV-A2.
- 6: **if** $\text{path_exists}((0, \mathbf{q}_1[0]), \mathbb{N} \times \mathcal{D}_1)$ **then**
- 7: $\{(n_0, \mathbf{q}_1[0]), (n_1, \mathbf{q}_1[1]), \dots, (n_{\tilde{N}-1}, \mathbf{q}_1[\tilde{N} - 1])\}$
 $:= \text{shortest_path}((0, \mathbf{q}_1[0]), \mathbb{N} \times \mathcal{D}_1)$
- 8: Obtain $\mathbf{Q}[\tilde{n}] = [\mathbf{q}_1[\tilde{n}], \hat{\mathbf{q}}_2[n_{\tilde{n}}]]$, $\tilde{n} = 0, 1, \dots, \tilde{N} - 1$
- 9: **return** $P^V = \{\mathbf{Q}[0], \mathbf{Q}[1], \dots, \mathbf{Q}[\tilde{N} - 1]\}$
- 10: **end if**
- 11: **end for**

Algorithm 3: PRFI for Static UE

input: $\bar{\mathcal{F}}_G, \mathbf{q}_{BS}, \mathbf{q}_{UE}, r_{CC}, r_{UE}^{\min}, c, C, \mathbf{Q}_0, v_{\max}$

- 1: $p_2 :=$ tentative path for UAV-2 via Algorithm 1
- 2: $P^V :=$ combined tentative path via Algorithm 2
- 3: For each $\mathbf{Q} \in P^V$, draw $\lfloor C/\tilde{N} \rfloor$ CPs $\rightarrow \mathcal{N}$
- 4: Construct a nearest-neighbor graph from \mathcal{N}
- 5: $P^{\text{PR}} := \text{shortest_path}(\mathbf{Q}_0, \{\mathbf{Q} : r_{UE}(\mathbf{Q}) \geq r_{UE}^{\min}\})$
- 6: Compute waypoints $\{(t_n, \mathbf{Q}(t_n))\}_n$ as in Sec. IV-C
- 7: **return** times and waypoints $\{(t_n, \mathbf{Q}(t_n))\}_n$

Along the lines of Sec. IV, the algorithm here is referred to PRFI for moving UE and also plans a tentative path first and then adapts PR to find a path in Q-space. However, the algorithm developed in this section significantly differs from the one in Sec. IV due to the different temporal dynamics of the problems they address: whereas in Sec. IV the UAVs must move at maximum speed to reach the destination as fast as possible, in the case of a moving UE, the time at which the UAVs must arrive at each waypoint is dictated by the trajectory of the UE. For this reason, the paths of the UE and UAVs will be handled by sampling their trajectories at a regular interval τ . Specifically, the path of the UE will be represented as $p_{\text{UE}} := \{\mathbf{q}_{\text{UE}}[0], \mathbf{q}_{\text{UE}}[1], \dots, \mathbf{q}_{\text{UE}}[N_{\text{UE}} - 1]\}$, where $\mathbf{q}_{\text{UE}}[n] = \mathbf{q}_{\text{UE}}(n\tau)$, $n = 0, \dots, N_{\text{UE}} - 1$. Similarly, the paths of the UAVs will be planned in such a way that each one is at a point of $\bar{\mathcal{F}}_G$ at every sampling instant. This requires that τ is small enough so that the UAVs can move from one grid point to any adjacent one in this time.

A. Planning the Tentative Path

As in Sec. IV, the focus will be on the case of two UAVs for simplicity and because $K = 2$ allows for reasonable solutions to (4). Recall that the closer the tentative path to the optimal combined path, the greater the optimality of the combined path returned by PR. Therefore, it is desirable that the tentative path approximately minimizes the adopted metric. In the case of

the outage time, this can be readily accomplished by planning the path of both UAVs separately along the lines of Sec. IV. However, when the metric is the one in (7), such an approach is not viable because the UE rate is a function of the positions of both UAVs. As noted in Sec. III, planning such a path jointly would be computationally prohibitive. Thus, with this metric, the tentative path will still be planned to minimize the outage time. PR will then optimize the path in Q-space to maximize the metric in (7).

1) *Path for UAV-2*: Given that the goal is to minimize the outage time, one would ideally like to *impose* that UAV-2 remains in the set of locations where it can provide r_{UE}^{\min} to the UE for a suitable location of UAV-1. Since this set generally changes over time and, therefore, such an approach need not be feasible, a reasonable alternative is to *encourage* UAV-2 to stay in these sets of locations by planning a path through an extended graph with properly weighted edges.

To construct such a graph, note that the set of candidate locations of UAV-2 is $\mathcal{N}_2 \triangleq \mathcal{R}(\mathbf{q}_{\text{BS}}, 2r_{\text{CC}}, r_{\text{CC}})$ and does not depend on the location of the UE. With $\tilde{\mathcal{N}}_2[n] \triangleq \{(n, \mathbf{q}) | \mathbf{q} \in \mathcal{N}_2\}$ denoting the set of extended nodes at time step n , the node set of the extended graph is $\tilde{\mathcal{N}}_2 \triangleq \cup_n \tilde{\mathcal{N}}_2[n]$. In contrast, the set of destinations $\mathcal{D}_2[n] \triangleq \mathcal{R}(\mathbf{q}_{\text{BS}}, 2r_{\text{CC}} + r_{\text{UE}}^{\min}, r_{\text{CC}} + r_{\text{UE}}^{\min}) \cap \mathcal{R}(\mathbf{q}_{\text{UE}}[n], r_{\text{UE}}^{\min})$, which comprises those locations where UAV-2 can provide r_{UE}^{\min} to the UE, does generally change over time as it depends on $\mathbf{q}_{\text{UE}}[n]$. The corresponding set of extended nodes at time step n is given by $\bar{\mathcal{D}}_2[n] \triangleq \{(n, \mathbf{q}) | \mathbf{q} \in \mathcal{D}_2[n]\} \subset \tilde{\mathcal{N}}_2[n] \subset \tilde{\mathcal{N}}_2$.

In this graph, nodes (n, \mathbf{q}) and (n', \mathbf{q}') are connected by an edge iff $n' = n + 1$ and $(\mathbf{q}', \mathbf{q}) \in \mathcal{E}_{\tilde{\mathcal{F}}_G}$. In this way, a path for UAV-2 is a sequence of extended nodes $(0, \mathbf{q}_2[0]), (1, \mathbf{q}_2[1]), \dots, (N_{\text{UE}} - 1, \mathbf{q}_2[N_{\text{UE}} - 1])$ where $(n, \mathbf{q}_2[n]) \in \tilde{\mathcal{N}}_2[n]$ and $(\mathbf{q}_2[n], \mathbf{q}_2[n + 1]) \in \mathcal{E}_{\tilde{\mathcal{F}}_G} \forall n$. The weight of an edge $((n, \mathbf{q}), (n', \mathbf{q}'))$, which captures the cost of traveling from (n, \mathbf{q}) to (n', \mathbf{q}') , is given by

$$w((n, \mathbf{q}), (n', \mathbf{q}')) = \begin{cases} 0 & \text{if } \mathbf{q} = \mathbf{q}', \mathbf{q}' \in \mathcal{D}_2[n'] \\ 1 & \text{if } \mathbf{q} \neq \mathbf{q}', \mathbf{q}' \in \mathcal{D}_2[n'] \\ w_p & \text{if } \mathbf{q}' \notin \mathcal{D}_2[n'], \end{cases} \quad (10)$$

where w_p is a large positive number that encourages UAV-2 to stay in $\bar{\mathcal{D}}_2[n]$ at time step n . Observe that, even when UAV-2 remains in these sets, the cost is greater if it moves.

A shortest path algorithm is used to find the path of UAV-2 from the extended node corresponding to the take-off location to any extended node in $\tilde{\mathcal{N}}_2[N_{\text{UE}} - 1]$. The procedure to find the path of UAV-2 is summarized as Algorithm 4.

2) *Path for UAV-1*: With the cost in (10), the number of time slots where UAV-2 is in a location that can provide r_{UE}^{\min} to the UE for a suitable location of UAV-1 is maximized. By suitable location it is meant that UAV-1 can provide $r_{\text{CC}} + r_{\text{UE}}^{\min}$ to UAV-2. Unfortunately, since the set of suitable locations for UAV-1 changes with n , it may not be possible for UAV-1 to be in a suitable location all the time. By finding a path for UAV-1 so that it stays within these sets as much as possible, the combined path will approximately minimize the outage time.

To this end, the path must be planned through an extended graph. Let $p_2 = \{\mathbf{q}_2[0], \mathbf{q}_2[1], \dots, \mathbf{q}_2[N_{\text{UE}} - 1]\}$ be the path

of UAV-2 returned by Algorithm 4. The set of candidate locations of UAV-1 at time step n is $\mathcal{N}_1[n] \triangleq \mathcal{R}(\mathbf{q}_{\text{BS}}, 2r_{\text{CC}}) \cap \mathcal{R}(\mathbf{q}_2[n], r_{\text{CC}})$ and the associated set of extended nodes is $\tilde{\mathcal{N}}_1[n] \triangleq \{(n, \mathbf{q}) | \mathbf{q} \in \mathcal{N}_1[n]\}$. The node set of the extended graph is therefore $\tilde{\mathcal{N}}_1 \triangleq \cup_n \tilde{\mathcal{N}}_1[n]$. On the other hand, the set of destinations of UAV-1 at time step n is given by $\mathcal{D}_1[n] \triangleq \mathcal{R}(\mathbf{q}_{\text{BS}}, 2r_{\text{CC}} + r_{\text{UE}}^{\min}) \cap \mathcal{R}(\mathbf{q}_2[n], r_{\text{CC}} + r_{\text{UE}}^{\min}) \subset \mathcal{N}_1[n]$.

As opposed to Sec. IV-A, UAV-2 cannot wait for UAV-1 since that would introduce an offset between a part of p_2 and p_{UE} . Nodes (n, \mathbf{q}) and (n', \mathbf{q}') are therefore connected by an edge iff $n' = n + 1$ and $(\mathbf{q}', \mathbf{q}) \in \mathcal{E}_{\tilde{\mathcal{F}}_G}$. This means that the path of UAV-1 in the extended graph will have the form $(0, \mathbf{q}_1[0]), (1, \mathbf{q}_1[1]), \dots, (N_{\text{UE}} - 1, \mathbf{q}_1[N_{\text{UE}} - 1])$, where $(n, \mathbf{q}_1[n]) \in \tilde{\mathcal{N}}_1[n]$ and $(\mathbf{q}_1[n], \mathbf{q}_1[n + 1]) \in \mathcal{E}_{\tilde{\mathcal{F}}_G} \forall n$. Similarly to UAV-2, the weight of the edge from (n, \mathbf{q}) to (n', \mathbf{q}') is given by (10) with $\mathcal{D}_1[n']$ in place of $\mathcal{D}_2[n']$.

The goal is, therefore, to find a path from the extended node corresponding to the take-off location to any node in $\tilde{\mathcal{N}}_1[N_{\text{UE}} - 1]$. Among such feasible paths, a shortest path algorithm picks the one that results in the lowest accumulated cost, hence the lowest outage time if w_p is sufficiently large.

Lifting. As in Sec. IV, no path for UAV-1 may exist for a given p_2 such that the combined path is feasible. Similarly to Sec. IV-A2, one can remedy this by lifting p_2 since this generally expands the sets of candidate locations of UAV-1. However, the lifting operator to be used here differs from the one in Sec. IV-A2 since the length of the lifted path must equal the length of p_2 and, consequently, the length of p_{UE} .

Consider an arbitrary path $p = \{\mathbf{q}[0], \mathbf{q}[1], \dots, \mathbf{q}[N - 1]\}$. Let $A(p) \triangleq \{\mathbf{q}[0], L(\mathbf{q}[0]), L(\mathbf{q}[1]), \dots, L(\mathbf{q}[N - 1])\}$, where L is defined in (8), be an operator that lifts each point and appends the first one at the beginning. Observe that the length of $A(p)$ equals the length of p plus 1. Also, let $A^{(1)}(p) \triangleq A(p)$ and $A^{(u)}(p) \triangleq A(A^{(u-1)}(p))$. On the other hand, let $Z(p) \triangleq \{\mathbf{q}[0], \mathbf{q}[1], \dots, \mathbf{q}[\bar{n} - 1], \mathbf{q}[\bar{n} + 1], \dots, \mathbf{q}[N - 1]\}$, where \bar{n} is the smallest n such that $\mathbf{q}[n] = \mathbf{q}[n + 1]$ and $\bar{n} = N - 1$ if $\mathbf{q}[n] \neq \mathbf{q}[n + 1]$ for all n . Observe that the length of $Z(p)$ equals the length of p minus 1. Also, $Z^{(1)}(p) \triangleq Z(p)$ and $Z^{(i)}(p) \triangleq Z(Z^{(i-1)}(p))$. Finally, let $\bar{L}^{(u)}(p) \triangleq Z^{(u)}(A^{(u)}(p))$ and observe that (i) the length of $\bar{L}^{(u)}(p)$ equals the length of p , and (ii), if p is a path where each pair of consecutive waypoints are adjacent in \mathcal{G} , the same holds for $\bar{L}^{(u)}(p)$.

As in Sec. IV-A2, the lifting operator is iteratively applied to p_2 until a path $\{\mathbf{q}_1[0], \mathbf{q}_1[1], \dots, \mathbf{q}_1[N_{\text{UE}} - 1]\}$ for UAV-1 is found. With u the number of required lifting steps, the tentative path is then $P^{\text{F}} = \{\mathbf{Q}[0], \dots, \mathbf{Q}[N_{\text{UE}} - 1]\}$, where $\mathbf{Q}[n] = \{\mathbf{q}_1[n], \hat{\mathbf{q}}_2[n]\}$ for $\{\hat{\mathbf{q}}_2[0], \dots, \hat{\mathbf{q}}_2[N_{\text{UE}} - 1]\} \triangleq \bar{L}^{(u)}(p_2)$. This procedure is summarized as Algorithm 5.

3) *Theoretical Guarantees*: As in Sec. IV-A3, it is possible to guarantee that the above iterative lifting procedure will eventually produce a feasible path.

Let h_{max} be the height of the lowest grid level that is higher than all obstacles and let $\tilde{\mathcal{F}}_G^{\text{max}} \triangleq \{\mathbf{q} \in \tilde{\mathcal{F}}_G : [0, 0, 1] \mathbf{q} = h_{\text{max}}\}$ be the grid level of height h_{max} . Let $\mathcal{C}(d_c) \triangleq \{[x, y, z]^T \in \mathbb{R}^3 : (x - x_{\text{BS}})^2 + (y - y_{\text{BS}})^2 \leq d_c^2\}$ be a cylinder of radius d_c centered at \mathbf{q}_{BS} and let $d_{c, \text{min}}$ be the smallest d_c such that $\tilde{\mathcal{F}}_G \subset \mathcal{C}(d_c)$ or, equivalently, the maximum horizontal distance from the BS to any point in $\tilde{\mathcal{F}}_G$.

Theorem 2: Suppose that $\mathbf{Q}_0 = [\mathbf{q}_{BS}, \mathbf{q}_{BS}]$ and let $p_2 = \{\mathbf{q}_2[0], \mathbf{q}_2[1], \dots, \mathbf{q}_2[N_{UE}-1]\}$ be the path of UAV-2 returned by Algorithm 4. If $h_{max} \leq c^{-1}(2r_{CC})$ and $d_{c,min} \leq c^{-1}(r_{CC})$, then Algorithm 5 will provide a feasible combined path.

Proof: See Appendix C. ■

It is also easy to see that, for a sufficiently large w_p , the tentative path is not only feasible but also optimal in terms of outage time if no lifting steps are required and UAV-1 remains at destination points throughout the entire path. When it comes to total transferred data, the tentative path will not generally be optimal, but can reasonably be expected to be similar to the optimal path in many cases.

B. Probabilistic Roadmaps with Feasible Initialization

The next step is to find a combined path around the tentative path that approximately optimizes the considered metric. Since the set of candidate CPs changes over time, an extended graph needs to be adopted. To operate on this graph, the PR algorithm in Sec. III will be generalized.

1) *Construction of the Node Set:* In addition to the CPs in the tentative path $P^F = \{\mathbf{Q}[0], \dots, \mathbf{Q}[N_{UE}-1]\}$, the algorithm draws $C \geq N_{UE}$ additional CPs. In particular, $\lfloor C/N_{UE} \rfloor$ CPs are drawn around each $\mathbf{Q}[n]$ as in Sec. IV-B1. With $\mathcal{N}[n]$ representing the set that contains $\mathbf{Q}[n]$ and the CPs drawn around $\mathbf{Q}[n]$, the set of extended nodes at time step n is given by $\tilde{\mathcal{N}}[n] \triangleq \{(n, \mathbf{Q}) | \mathbf{Q} \in \mathcal{N}[n]\}$.

2) *Construction of the Edge Set:* Two extended nodes (n, \mathbf{Q}) and (n', \mathbf{Q}') are connected by an edge iff $n' = n + 1$, $(\mathbf{q}_1, \mathbf{q}'_1) \in \mathcal{E}_{\mathcal{F}_G}$, and $(\mathbf{q}_2, \mathbf{q}'_2) \in \mathcal{E}_{\mathcal{F}_G}$, where $\mathbf{Q} = [\mathbf{q}_1, \mathbf{q}_2]$ and $\mathbf{Q}' = [\mathbf{q}'_1, \mathbf{q}'_2]$. The edge weights depend on the metric to be optimized. To minimize the outage time, one can set

$$w((n, \mathbf{Q}), (n', \mathbf{Q}')) = \begin{cases} 0 & \text{if } \mathbf{Q} = \mathbf{Q}', r_{UE}(\mathbf{Q}') \geq r_{UE}^{\min} \\ 1 & \text{if } \mathbf{Q} \neq \mathbf{Q}', r_{UE}(\mathbf{Q}') \geq r_{UE}^{\min} \\ w_p & \text{if } r_{UE}(\mathbf{Q}') < r_{UE}^{\min}, \end{cases} \quad (11)$$

where w_p is again a large positive number. When it comes to the total transferred data, observe that the integral in (7) can be discretized as

$$J(\mathcal{T}) \approx -\tau \sum_{n=0}^{N_{UE}-1} r_{UE}(\mathbf{Q}[n], \mathbf{q}_{UE}[n]). \quad (12)$$

Since a shortest path algorithm minimizes the sum of the weights of the edges in a path, one can therefore set $w((n, \mathbf{Q}), (n', \mathbf{Q}')) = -r_{UE}(\mathbf{Q}', \mathbf{q}_{UE}[n'])$.

3) *Path Planning in Q-Space:* A shortest-path algorithm is then used to find the path $P^{PR} = \{\mathbf{Q}[0], \mathbf{Q}[1], \dots, \mathbf{Q}[N_{UE}-1]\}$ of the UAVs in the extended graph from \mathbf{Q}_0 to an extended node in $\tilde{\mathcal{N}}[N_{UE}-1]$ that results in the lowest accumulated cost. This differs from standard PR, which finds a shortest path through a nearest-neighbor graph.

C. From the Waypoint Sequence to the Trajectory

As described at the beginning of Sec. V, the produced path for the UAVs is sampled at regular intervals τ . Thus, given P^{PR} , the final trajectory $\mathcal{T}^{PR} = \{\mathbf{Q}(t), t \geq 0\}$ satisfies

Algorithm 4: Tentative Path UAV-2, Moving UE

input: $\bar{\mathcal{F}}_G, \mathbf{q}_{BS}, r_{CC}, r_{UE}^{\min}, \mathbf{q}_2[0]$,
 $p_{UE} = \{\mathbf{q}_{UE}[0], \mathbf{q}_{UE}[1], \dots, \mathbf{q}_{UE}[N_{UE}-1]\}$
1: Find candidate locations of UAV-2
 $\rightarrow \mathcal{N}_2[n] = \mathcal{R}(\mathbf{q}_{BS}, 2r_{CC}, r_{CC})$
2: Find destinations of UAV-2 $\rightarrow \mathcal{D}_2[n] =$
 $\mathcal{R}(\mathbf{q}_{BS}, 2r_{CC} + r_{UE}^{\min}, r_{CC} + r_{UE}^{\min}) \cap \mathcal{R}(\mathbf{q}_{UE}[n], r_{UE}^{\min})$
3: Construct extended graph \mathcal{G}_3 with weights (10)
4: $p_2 := \text{shortest_path}((0, \mathbf{q}_2[0]), \mathcal{N}_2[N_{UE}-1])$
5: **return** $p_2 = \{\mathbf{q}_2[0], \mathbf{q}_2[1], \dots, \mathbf{q}_2[N_{UE}-1]\}$

Algorithm 5: Tentative Path UAV-1, Moving UE

input: $\bar{\mathcal{F}}_G, \mathbf{q}_{BS}, r_{CC}, r_{UE}^{\min}, \mathbf{q}_1[0]$,
 $p_2 = \{\mathbf{q}_2[0], \mathbf{q}_2[1], \dots, \mathbf{q}_2[N_{UE}-1]\}$
1: **for** $u = 0, 1, \dots$ **do**
2: $\{\hat{\mathbf{q}}_2[0], \hat{\mathbf{q}}_2[1], \dots, \hat{\mathbf{q}}_2[N_{UE}-1]\} := \bar{L}^{(u)}(p_2)$
3: Find candidate locations of UAV-1
 $\rightarrow \mathcal{N}_1[n] = \mathcal{R}(\mathbf{q}_{BS}, 2r_{CC}) \cap \mathcal{R}(\hat{\mathbf{q}}_2[n], r_{CC})$
4: Find destinations of UAV-1
 $\rightarrow \mathcal{D}_1[n] = \mathcal{R}(\mathbf{q}_{BS}, 2r_{CC} + r_{UE}^{\min}) \cap \mathcal{R}(\hat{\mathbf{q}}_2[n], r_{CC} + r_{UE}^{\min})$
5: Form extended nodes $\rightarrow \tilde{\mathcal{N}}_1[n] \triangleq \{(n, \mathbf{q}) | \mathbf{q} \in \mathcal{N}_1[n]\}$
6: Construct extended graph \mathcal{G}_4 with weights given by Sec. V-A2.
7: **if** $\text{path_exists}((0, \mathbf{q}_1[0]), \tilde{\mathcal{N}}_1[N_{UE}-1])$ **then**
8: $\{(0, \mathbf{q}_1[0]), \dots, (N_{UE}-1, \mathbf{q}_1[N_{UE}-1])\}$
 $= \text{shortest_path}((0, \mathbf{q}_1[0]), \tilde{\mathcal{N}}_1[N_{UE}-1])$
9: Obtain $\mathbf{Q}[n] = [\mathbf{q}_1[n], \hat{\mathbf{q}}_2[n]]$, $n = 0, 1, \dots, N_{UE}-1$
10: **Return** $P^F = \{\mathbf{Q}[0], \mathbf{Q}[1], \dots, \mathbf{Q}[N_{UE}-1]\}$
11: **end if**
12: **end for**

Algorithm 6: PRFI for Moving UE

input: $\bar{\mathcal{F}}_G, \mathbf{q}_{BS}, r_{CC}, r_{UE}^{\min}, c, C, \mathbf{Q}_0, \tau, p_{UE}$ of length N_{UE}
1: $p_2 :=$ tentative path for UAV-2 via Algorithm 4
2: $P^F :=$ combined tentative path via Algorithm 5
3: For each $\mathbf{Q}[n] \in P^F$, draw $\lfloor C/N_{UE} \rfloor$ CPs $\rightarrow \tilde{\mathcal{N}}[n]$
4: Construct extended graph with weights as in Sec. V-B
5: $P^{PR} := \text{shortest_path}((0, \mathbf{Q}_0), \tilde{\mathcal{N}}[N_{UE}-1])$
6: **return** times and waypoints $\{(n\tau, \mathbf{Q}[n])\}_n$.

$\mathbf{Q}(n\tau) = \mathbf{Q}[n], n = 0, \dots, N_{UE}-1$. As indicated earlier, the position of the UAVs at intermediate time instants is determined by the flight controller.

The complete procedure is summarized as Algorithm 6.

VI. NUMERICAL EXPERIMENTS

This section presents numerical results that validate the efficacy and assess the performance of the proposed PRFI algorithms. The developed simulator, the simulation code, and some videos can be found at https://github.com/uiano/pr_for_relay_path_planning.

A. Simulation Setup

In all experiments, the relevant performance metric is estimated using the Monte Carlo (MC) method with 400 realizations. The simulation scenario consists of an urban environment with 25 buildings in a region $\mathcal{S} = [0, 500] \times [0, 500] \times [0, 100]$ m. After setting the minimum and maximum flight heights respectively to 12.5 m and $h_{\text{top}} = 87.5$ m, a $12 \times 12 \times 8$ rectangular flight grid $\bar{\mathcal{F}}_G$ is constructed. The UAVs start at $\mathbf{Q}_0 = [\mathbf{q}_{\text{BS}}, \mathbf{q}_{\text{BS}}]$, where $\mathbf{q}_{\text{BS}} = [20, 470, 0]^\top$. For generating \mathbf{q}_{UE} at each MC realization, the distance $d_{\text{BS}}^{\text{UE}} = \|\mathbf{q}_{\text{UE}} - \mathbf{q}_{\text{BS}}\|$ is first generated uniformly at random in the interval $[\hat{d}_{\text{BS}}^{\text{UE}}, \check{d}_{\text{BS}}^{\text{UE}}]$. Unless otherwise stated, $\hat{d}_{\text{BS}}^{\text{UE}} = 50$ m and $\check{d}_{\text{BS}}^{\text{UE}} = 650$ m. Subsequently, \mathbf{q}_{UE} is drawn uniformly at random among the points that (i) are outside the buildings, (ii) are at a distance $d_{\text{BS}}^{\text{UE}}$ from \mathbf{q}_{BS} , and (iii) satisfy $c(\mathbf{q}_{\text{BS}}, \mathbf{q}_{\text{UE}}) \leq r_{\text{UE}}^{\text{min}}$.

The trajectories of the UAVs are constrained by the maximum speed of $v_{\text{max}} = 7$ m/s and the need for maintaining a minimum UAV rate of $r_{\text{CC}} = 200$ kbps.

The BS and UAVs transmit signals of carrier frequency 6 GHz, bandwidth 20 MHz, and transmit power 17 dBm. An antenna gain of 12 dBi is used at both the transmit and receive sides to simulate the beamforming gain of an antenna array. The channel is determined by c , which is generated using the tomographic channel model [34], [35] with an absorption of 1 dB/m inside the buildings and 0 dB/m outside. The noise power is -97 dBm.

Unless otherwise stated, the proposed PRFI algorithms use $C = 2000$ CPs and 100 neighbors.

B. Static UE

This section studies the performance of the proposed PRFI algorithm for static UE. Throughout this section, all buildings have a height of 40 m.

Due to the presence of buildings, no algorithm in the literature that the authors are aware of can directly accommodate the considered simulation setup. Instead, three benchmarks will be considered: In Benchmark 1, a single UAV takes off at \mathbf{q}_{BS} vertically to the height of h_{top} and then moves horizontally in a straight line towards the point $([x_{\text{BS}}, y_{\text{BS}}, h_{\text{top}}]^\top + [x_{\text{UE}}, y_{\text{UE}}, h_{\text{top}}]^\top)/2$, which is equidistant from the BS and UE. In Benchmark 2, two UAVs lift off at the BS to the height of h_{top} . Then UAV-1 moves to $(2/3)[x_{\text{BS}}, y_{\text{BS}}, h_{\text{top}}]^\top + (1/3)[x_{\text{UE}}, y_{\text{UE}}, h_{\text{top}}]^\top$ whereas UAV-2 moves to $(1/3)[x_{\text{BS}}, y_{\text{BS}}, h_{\text{top}}]^\top + (2/3)[x_{\text{UE}}, y_{\text{UE}}, h_{\text{top}}]^\top$. Benchmark 3 is similar to Benchmark 2, but UAV-1 remains at $[x_{\text{BS}}, y_{\text{BS}}, h_{\text{top}}]^\top$ after lifting off whereas UAV-2 follows a horizontal straight line to $[x_{\text{UE}}, y_{\text{UE}}, h_{\text{top}}]^\top$. Recall that, under the hypotheses of Proposition 1, the resulting path is always feasible and yields a finite cost. All three benchmarks stop at the point of their trajectories where the UE rate is maximum.

Fig. 3 compares the mean instantaneous rate $\mathbb{E}[r_{\text{UE}}(\mathbf{Q}(t))]$ of the considered algorithms. Since all UAVs start from the BS, the initial rate is the same for all algorithms. Although Benchmarks 1 and 2 do not reach the target rate, Benchmark 3 does succeed, as dictated by Proposition 1. PRFI (Tentative), which corresponds to the trajectory produced by Algorithm 2,

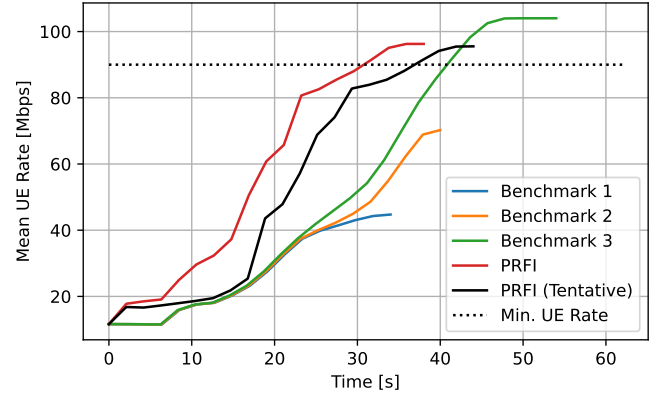


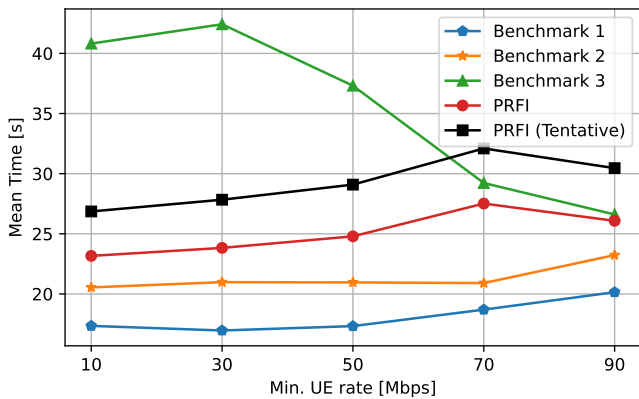
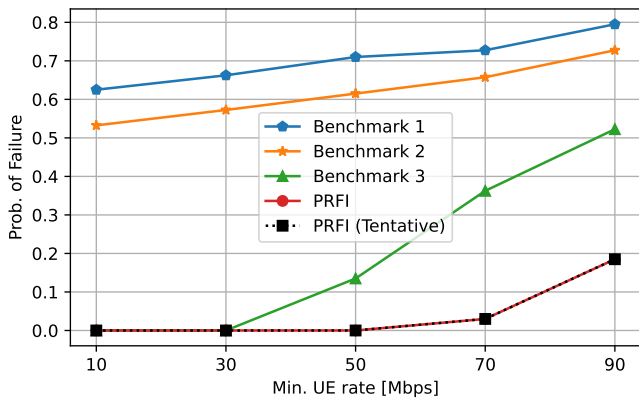
Fig. 3: Expected UE rate $\mathbb{E}[r_{\text{UE}}(\mathbf{Q}(t))]$ vs. t . The proposed algorithm is the first to attain the target rate $r_{\text{UE}}^{\text{min}}$ ($r_{\text{UE}}^{\text{min}} = 90$ Mbps, $[\hat{d}_{\text{BS}}^{\text{UE}}, \check{d}_{\text{BS}}^{\text{UE}}] = [230, 270]$ m).

is already significantly faster than Benchmark 3, which corroborates the efficacy of the tentative path. PRFI, which returns the result of applying PR to the tentative path, is even faster than PRFI (Tentative). This validates the adoption of PR.

The second experiment studies the influence of $r_{\text{UE}}^{\text{min}}$ on the expectation of the connection time, which is the cost in (5). To this end, Fig. 4 plots $\mathbb{E}[T_c(\mathcal{T})|T_c(\mathcal{T}) < \infty]$ and the probability of failure vs. $r_{\text{UE}}^{\text{min}}$. The notation $\mathbb{E}[T_c(\mathcal{T})|T_c(\mathcal{T}) < \infty]$ indicates that only those MC realizations where $r_{\text{UE}}^{\text{min}}$ is attained are considered in the MC average. The probability of failure is defined as the ratio between the number of MC realizations in which $r_{\text{UE}}(\mathbf{Q}(t)) < r_{\text{UE}}^{\text{min}} \forall t$ and the total number of realizations. It is mainly determined by the relation between $d_{\text{BS}}^{\text{UE}}$ and $r_{\text{UE}}^{\text{min}}$.

Observe that Benchmarks 1 and 2 have the lowest connection time. This is because they only succeed in the easiest MC realizations, as corroborated by their very high probability of failure. Benchmark 3, is outperformed by the proposed algorithm both in terms of probability of failure and mean connection time. Benchmark 3 also provides a null probability of failure until $r_{\text{UE}}^{\text{min}} \approx 30$ Mbps, in which case the hypotheses of Proposition 1 no longer hold. Note as well that PRFI is considerably faster than PRFI (Tentative) in all scenarios. This again corroborates the efficacy of the proposed approach, where a feasible tentative path is improved using PR.

The next experiment studies the influence of the distance $d_{\text{BS}}^{\text{UE}} = \|\mathbf{q}_{\text{BS}} - \mathbf{q}_{\text{UE}}\|$ on the connection time and probability of failure. To this end, Fig. 5 plots $\mathbb{E}[T_c(\mathcal{T})|T_c(\mathcal{T}) < \infty]$ and the probability of failure vs. $d_{\text{BS}}^{\text{UE}}$. In this figure, for a given value d on the x-axis, $\hat{d}_{\text{BS}}^{\text{UE}} = d - 20$ m and $\check{d}_{\text{BS}}^{\text{UE}} = d + 20$ m. Overall, it is seen that both the mean connection time and probability of failure increase with $d_{\text{BS}}^{\text{UE}}$. However, in Fig. 5b, the probability of failure of Benchmarks 1 and 2 initially decreases. This is because the MC realizations with good direct channel gains between the BS and UE are discarded, which promotes that the BS and UE lie at opposite sides of the buildings when $d_{\text{BS}}^{\text{UE}}$ is low. Finally, observe that PRFI has the lowest connection time and probability of failure for all the considered values of $d_{\text{BS}}^{\text{UE}}$.

(a) Mean time to connect vs. r_{UE}^{\min} .(b) Probability of failure vs. r_{UE}^{\min} .Fig. 4: Mean connection time and probability of failure vs. r_{UE}^{\min} .

C. Moving UE

This section studies the performance of PRFI for moving UE; cf. Sec. V. The objective is to maximize the total data transferred to the UE, which follows a random trajectory of 300 seconds at a speed of 2 m/s and starting at an initial position generated as the UE location in Sec. VI-B. Throughout, the height of each building at each MC realization is uniformly distributed between 20 m and 75 m.

An example of such a trajectory is shown in Fig. 6.

The following two benchmarks are considered: Benchmark 3 introduced in Sec. VI-B is adapted to serve a moving UE. In particular, both UAVs take off vertically from \mathbf{q}_{BS} to h_{top} . After that, UAV-1 remains at $[x_{BS}, y_{BS}, h_{top}]$ whereas, at every time step, UAV-2 flies to the adjacent grid point that is nearest to the UE. Benchmark 4 is a modified version of PRFI for static UE where, for every N_{replan} time steps, the UAVs are given the next N_{known} locations of the UE and a combined path that approximately minimizes the outage time in the next N_{known} time steps is found; cf. Appendix D for details. Here, $N_{replan} = 15$ and $N_{known} = 17$.

Fig. 7 plots the mean UE rate vs. time. Observe that PRFI (Tentative) attains r_{UE}^{\min} before PRFI. However, the latter results in a higher rate. This is consistent with the fact that PRFI (Tentative) aims at minimizing outage time whereas PRFI

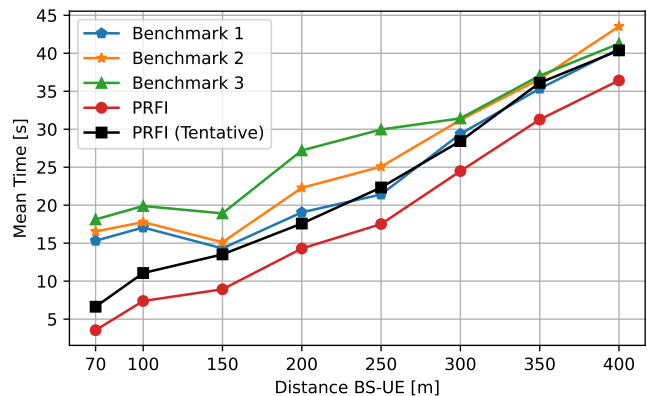
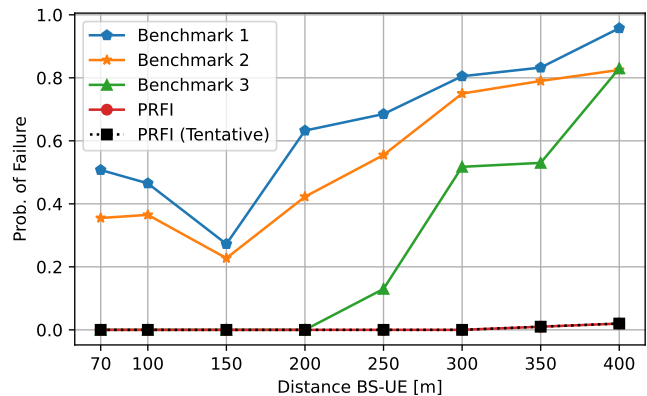
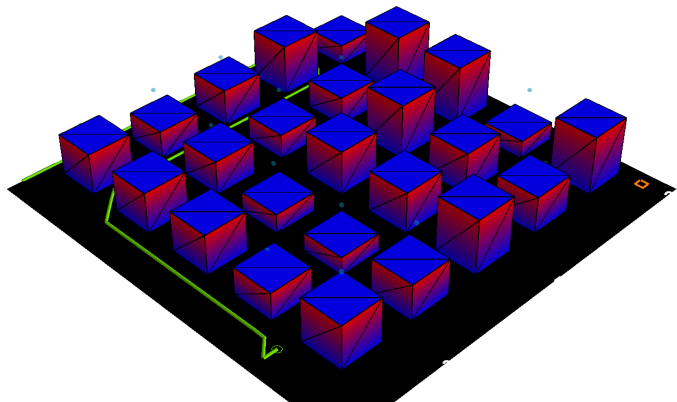
(a) Mean time to connect vs. mean $\|\mathbf{q}_{BS} - \mathbf{q}_{UE}\|$.(b) Probability of failure vs. mean $\|\mathbf{q}_{BS} - \mathbf{q}_{UE}\|$.Fig. 5: Mean connection time and probability of failure vs. mean $\|\mathbf{q}_{UE} - \mathbf{q}_{BS}\|$ ($r_{UE}^{\min} = 90$ Mbps).

Fig. 6: An example of a trajectory of a moving UE.

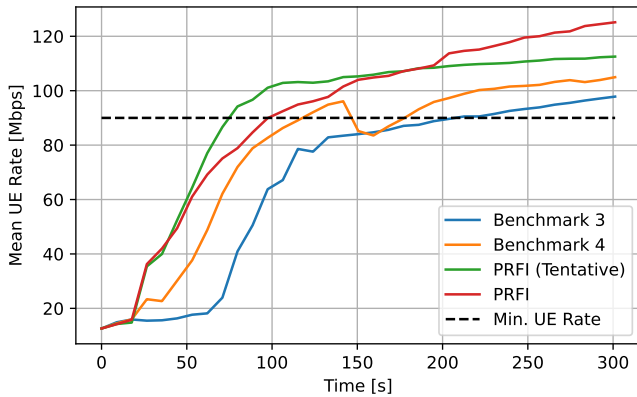


Fig. 7: Mean UE rate vs. time. $r_{\text{UE}}^{\min} = 90$ Mbps.

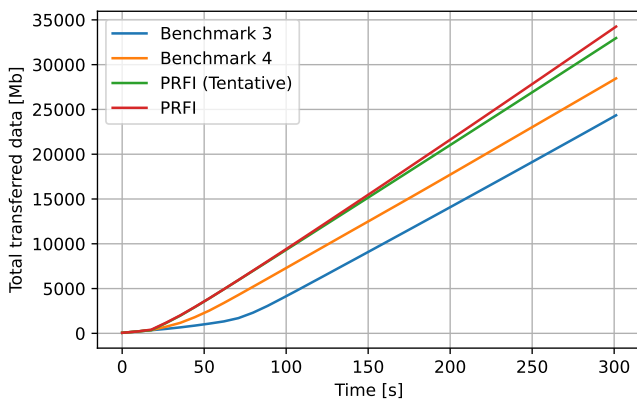


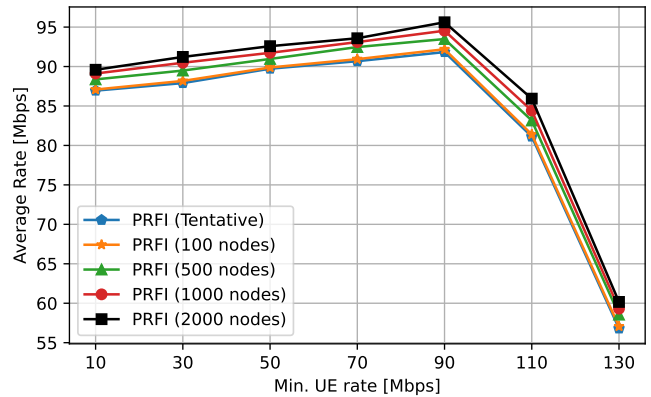
Fig. 8: Total transferred data vs. the time horizon T ($r_{\text{UE}}^{\min} = 60$ Mbps, $\hat{d}_{\text{BS}}^{\text{UE}} = 130$ m and $\hat{d}_{\text{BS}}^{\text{UE}} = 170$ m).

pursues the maximization of the total transferred data. The benchmarks are widely outperformed even by PRFI (Tentative). The sudden drop at around 140 s for Benchmark 4 is due to a replanning step.

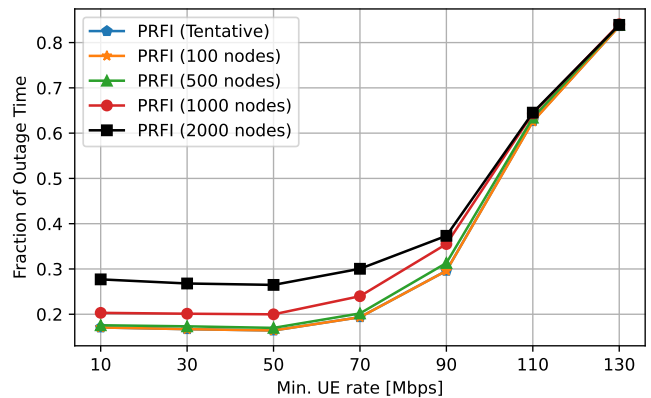
Fig. 8 plots the total transferred data vs. the time horizon T . The greatest slope, offered by PRFI, showcases the fact that it achieves the greatest rate. As a result, the margin by which it outperforms its competitors will increase as time progresses.

To investigate how to set the parameters of PRFI, Fig. 9 plots the average UE rate and fraction of outage time vs. r_{UE}^{\min} for different numbers C of drawn CPs in the PR step. The fraction of outage time is defined as the fraction of time where $r_{\text{UE}}(Q(t), q_{\text{UE}}(t)) \leq r_{\text{UE}}^{\min}$. To make differences between parameter values more conspicuous, an infinite building absorption is adopted.

As expected, the greater C , the higher the average UE rate. This is because using more CPs confers more freedom to PR, which targets maximizing rate. However, this increased optimality in terms of rate naturally entails a sacrifice in terms of outage time. Notice also the diminishing returns of increasing C : for example, the difference between $C = 100$ and $C = 1000$ is much more significant than the difference between $C = 1000$ and $C = 2000$. This means that computational complexity may be significantly reduced at the cost of



(a) Average UE rate vs. r_{UE}^{\min} .



(b) Fraction of outage time vs. r_{UE}^{\min} .

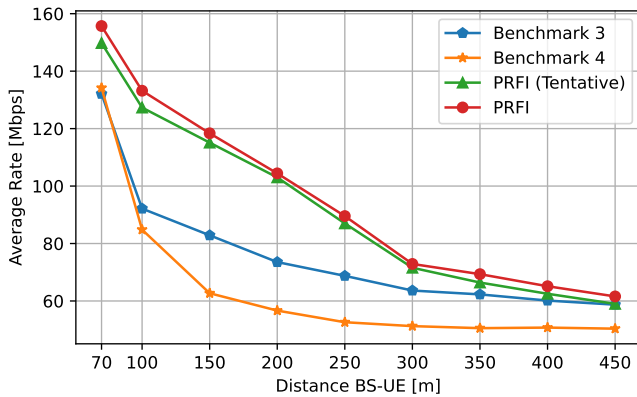
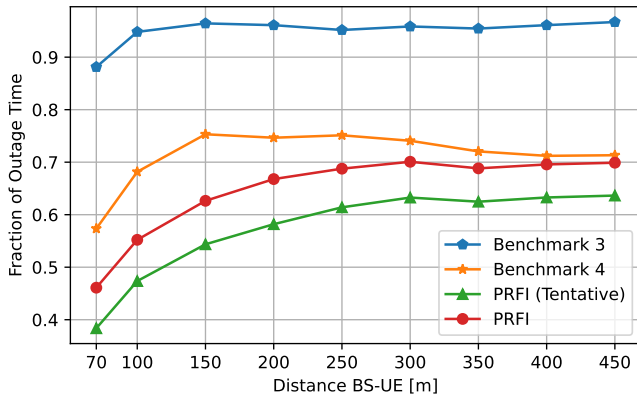
Fig. 9: Performance metrics vs. r_{UE}^{\min} of the proposed PRFI (800 MC realizations).

a mild decrease in performance.

To understand the influence of r_{UE}^{\min} , observe that the optimal path does not depend on this parameter. However, among the set of suboptimal paths, the one chosen by PRFI does depend on r_{UE}^{\min} because this parameter is used when generating the tentative path. Thus, it is important to properly set this parameter to reduce suboptimality as much as possible. To this end, observe from Fig. 9a that the average UE rate increases slowly when r_{UE}^{\min} is below a certain value. Above this value, the average UE rate decreases quickly. This suggests that it is preferable to select a reasonably small r_{UE}^{\min} in practice.

Fig. 10 aims at analyzing the influence of the initial $d_{\text{BS}}^{\text{UE}}$ on performance. For a given value d on the x-axis, $\hat{d}_{\text{BS}}^{\text{UE}} = d - 20$ m and $\hat{d}_{\text{BS}}^{\text{UE}} = d + 20$ m. As expected, PRFI provides the highest average UE rate and PRFI (Tentative) obtains the lowest fraction of outage time. PRFI still has a lower fraction of outage time than the benchmarks while PRFI (Tentative) achieves higher average rates than the benchmarks. These observations provide further empirical support for the adopted strategy and quality of the tentative path.

The final experiment studies the influence of the environment. To this end, Fig. 11 depicts the average UE rate and the fraction of outage time vs. the mean building height. For each h on the horizontal axis, the height of each building at

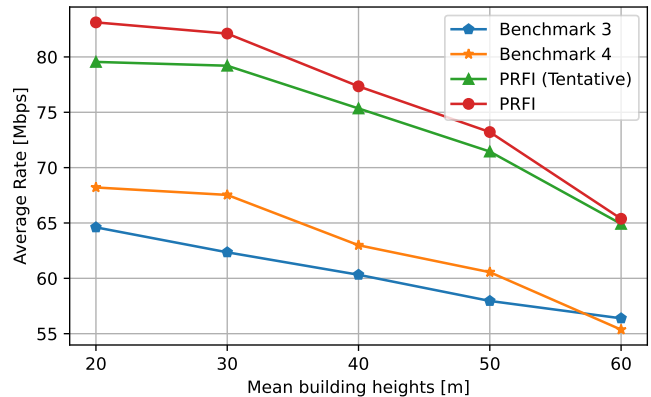
(a) Average UE rate vs. initial d_{BS}^{UE} .(b) Fraction of outage time vs. initial d_{BS}^{UE} .Fig. 10: Influence of the initial d_{BS}^{UE} on performance (800 realizations, $r_{UE}^{\min} = 110$ Mbps).

each MC realization is uniformly distributed between $h - 20$ m and $h + 20$ m. As expected, a greater height of the buildings results in a performance degradation. This is because building size constrains the possible trajectories and impair the propagation conditions by decreasing channel gain, which limits the locations where the UAVs can provide r_{UE}^{\min} to the UE and the CPs where the UAVs receive r_{CC} . Despite that fact, the proposed algorithm widely outperforms the benchmarks.

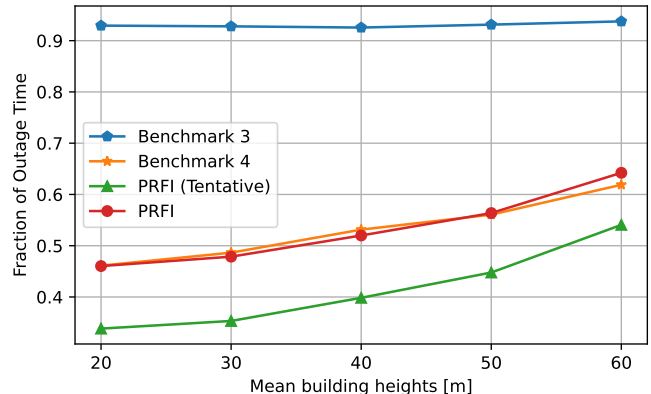
VII. CONCLUSIONS

This paper developed a framework for path planning of multiple aerial relays that approximately optimize communication metrics while accommodating arbitrary constraints on the flight region. The idea is to build upon the celebrated PR algorithm, which finds a shortest path through a random graph of CPs. To cope with the need for a large number of CPs in plain PR, a modification was proposed in which the CPs are drawn around a tentative path. This approach was applied to serve both a static and a moving user with two aerial relays. To this end, heuristic rules leading to tentative paths with theoretical guarantees were proposed. Numerical results demonstrate the merits of the proposed algorithms.

Future work will develop algorithms with more than two aerial relays and will investigate alternative sampling strategies



(a) Average UE rate vs. building height.



(b) Fraction of outage time vs. building height.

Fig. 11: Experiment with mean building height. $r_{UE}^{\min} = 100$ Mbps.

for PR. Another interesting direction is to plan the trajectories of UAVs to collect data from wireless sensors in urban environments.

REFERENCES

- [1] P. Q. Viet and D. Romero, "Aerial base station placement: A tutorial introduction," *IEEE Commun. Mag.*, vol. 60, no. 5, pp. 44–49, 2022.
- [2] D. Romero, P. Q. Viet, and R. Shrestha, "Aerial base station placement via propagation radio maps," *IEEE Trans. Commun.*, 2024.
- [3] J. Wang, X. Zhou, H. Zhang, and D. Yuan, "Joint trajectory design and power allocation for UAV assisted network with user mobility," *IEEE Trans. Veh. Technol.*, vol. 72, no. 10, pp. 13173–13189, May 2023.
- [4] Q. Hou, Y. Cai, Q. Hu, M. Lee, and G. Yu, "Joint resource allocation and trajectory design for multi-UAV systems with moving users: Pointer network and unfolding," *IEEE Trans. Wireless Commun.*, vol. 22, no. 5, pp. 3310–3323, Nov. 2023.
- [5] H. Wang, G. Ren, J. Chen, G. Ding, and Y. Yang, "Unmanned aerial vehicle-aided communications: Joint transmit power and trajectory optimization," *IEEE Wireless Commun. Lett.*, vol. 7, no. 4, pp. 522–525, 2018.
- [6] K. Anazawa, P. Li, T. Miyazaki, and S. Guo, "Trajectory and data planning for mobile relay to enable efficient internet access after disasters," in *Proc. IEEE Global Commun. Conf.*, 2015, pp. 1–6.
- [7] N. Zhao, W. Lu, M. Sheng, Y. Chen, J. Tang, F. R. Yu, and K. Wong, "UAV-assisted emergency networks in disasters," *IEEE Wireless Commun.*, vol. 26, no. 1, pp. 45–51, Feb. 2019.
- [8] S. Zhang, H. Zhang, Q. He, K. Bian, and L. Song, "Joint trajectory and power optimization for uav relay networks," *IEEE Commun. Lett.*, vol. 22, no. 1, pp. 161–164, Oct. 2018.

- [9] X. Jiang, Z. Wu, Z. Yin, W. Yang, and Z. Yang, "Trajectory and communication design for UAV-relayed wireless networks," *IEEE Wireless Commun. Lett.*, vol. 8, no. 6, pp. 1600–1603, Jul. 2019.
- [10] Q. Chen, "Joint trajectory and resource optimization for UAV-enabled relaying systems," *IEEE Access*, vol. 8, pp. 24108–24119, Jan. 2020.
- [11] Z. Sun, D. Yang, L. Xiao, L. Cuthbert, F. Wu, and Y. Zhu, "Joint energy and trajectory optimization for UAV-enabled relaying network with multi-pair users," *IEEE Trans. Cogn. Commun. Netw.*, vol. 7, no. 3, pp. 939–954, Dec. 2021.
- [12] J. Chen, U. Mitra, and D. Gesbert, "Optimal UAV relay placement for single user capacity maximization over terrain with obstacles," in *Proc. IEEE Workshop Signal Process. Adv. Wirel. Commun.*, Jul. 2019, pp. 1–5.
- [13] J. Chen, U. Mitra, and D. Gesbert, "3D urban UAV relay placement: Linear complexity algorithm and analysis," *IEEE Trans. Wireless Commun.*, vol. 20, no. 8, pp. 5243–5257, Mar. 2021.
- [14] P. Yi, L. Zhu, L. Zhu, Z. Xiao, Z. Han, and X. Xia, "Joint 3D positioning and power allocation for UAV relay aided by geographic information," *IEEE Trans. Wireless Commun.*, vol. 21, no. 10, pp. 8148–8162, Apr. 2022.
- [15] H. Asano, H. Okada, C. B. Naila, and M. Katayama, "Flight model using Voronoi tessellation for a delay-tolerant wireless relay network using drones," *IEEE Access*, vol. 9, pp. 13064–13075, 2021.
- [16] X. Wang, M. Yi, J. Liu, Y. Zhang, M. Wang, and B. Bai, "Cooperative data collection with multiple UAVs for information freshness in the internet of things," *IEEE Trans. Commun.*, vol. 71, no. 5, pp. 2740–2755, Mar. 2023.
- [17] G. Zhang, H. Yan, Y. Zeng, M. Cui, and Y. Liu, "Trajectory optimization and power allocation for multi-hop UAV relaying communications," *IEEE Access*, vol. 6, pp. 48566–48576, 2018.
- [18] G. Zhang, X. Ou, M. Cui, Q. Wu, S. Ma, and W. Chen, "Cooperative UAV enabled relaying systems: Joint trajectory and transmit power optimization," *IEEE Trans. Green Commun. Netw.*, vol. 6, no. 1, pp. 543–557, 2022.
- [19] Y. Zeng, R. Zhang, and T. J. Lim, "Throughput maximization for UAV-enabled mobile relaying systems," *IEEE Trans. Commun.*, vol. 64, no. 12, pp. 4983–4996, Dec. 2016.
- [20] M. Mahmood, Y. Yuan, and T. Le-Ngoc, "Multiple UAV-assisted cooperative DF relaying in multi-user massive MIMO IoT systems," *arXiv preprint arXiv:2404.03068*, 2024.
- [21] L. Liu, S. Zhang, and R. Zhang, "CoMP in the sky: UAV placement and movement optimization for multi-user communications," *IEEE Trans. Commun.*, vol. 67, no. 8, pp. 5645–5658, Aug. 2019.
- [22] J. Wu, L. Li, and L. Du, "UAV-assisted relaying transmission design and optimization for high-speed moving sources," *IEEE Access*, vol. 8, pp. 195857–195869, Oct. 2020.
- [23] T. Liu, M. Cui, G. Zhang, Q. Wu, X. Chu, and J. Zhang, "3D trajectory and transmit power optimization for UAV-enabled multi-link relaying systems," *IEEE Trans. Green Commun. Netw.*, vol. 5, no. 1, pp. 392–405, Dec. 2021.
- [24] H. Ghazzai, M. Ben-Ghorbel, A. Kessler, and M. J. Hossain, "Trajectory optimization for cooperative dual-band UAV swarms," in *Proc. IEEE Global Commun. Conf.*, 2018, pp. 1–7.
- [25] J. Lee and V. Friderikos, "Trajectory planning for multiple UAVs in UAV-aided wireless relay network," in *Proc. IEEE Int. Conf. Commun.*, 2022, pp. 1–6.
- [26] E. Yanmaz, "Positioning aerial relays to maintain connectivity during drone team missions," *Ad Hoc Networks*, vol. 128, pp. 102800, 2022.
- [27] S. Hong, S. U. Lee, X. Huang, M. Khonji, R. Alyassi, and B. C. Williams, "An anytime algorithm for chance constrained stochastic shortest path problems and its application to aircraft routing," in *Proc. IEEE Int. Conf. Robot. Autom.*, Oct. 2021, pp. 475–481.
- [28] H. Yang, J. Zhang, S. H. Song, and K. B. Lataief, "Connectivity-aware UAV path planning with aerial coverage maps," in *Proc. IEEE Wireless Commun. Netw. Conf.*, 2019, pp. 1–6.
- [29] L. E. Kavrakli, P. Svestka, J. C. Latombe, and M. H. Overmars, "Probabilistic roadmaps for path planning in high-dimensional configuration spaces," *IEEE Trans. Robot. Autom.*, vol. 12, no. 4, pp. 566–580, 1996.
- [30] O. V. P. Arista, O. R. V. Barona, and R. S. Nuñez-Cruz, "Development of an efficient path planning algorithm for indoor navigation," in *Int. Conf. Electr. Eng., Comput. Sci. Automat. Control*, 2021, pp. 1–6.
- [31] D. Romero and S.-J. Kim, "Radio map estimation: A data-driven approach to spectrum cartography," *IEEE Signal Process. Mag.*, vol. 39, no. 6, pp. 53–72, 2022.
- [32] J. Chen and D. Gesbert, "Optimal positioning of flying relays for wireless networks: A LOS map approach," in *Proc. IEEE Int. Conf.*, Paris, France, May 2017, pp. 1–6.
- [33] A. A. Khuwaja, Y. Chen, and G. Zheng, "Effect of user mobility and channel fading on the outage performance of UAV communications," *IEEE Wireless Commun. Lett.*, vol. 9, no. 3, pp. 367–370, Nov. 2020.
- [34] N. Patwari and P. Agrawal, "NeSh: a joint shadowing model for links in a multi-hop network," in *Proc. IEEE Int. Conf. Acoust., Speech, Signal Process.*, Las Vegas, NV, Mar. 2008, pp. 2873–2876.
- [35] N. Patwari and P. Agrawal, "Effects of correlated shadowing: Connectivity, localization, and RF tomography," in *Proc. Int. Conf. Info. Process. Sensor Networks*, St. Louis, MO, Apr. 2008, pp. 82–93.

APPENDIX A PROOF OF THEOREM 1

Let $p_2 \triangleq \{\mathbf{q}_2[0], \mathbf{q}_2[1], \dots, \mathbf{q}_2[N_0 - 1]\}$ be the path for UAV-2 returned by Algorithm 1. Observe that, for a given h_{\max} , there is a maximum number of times that p_2 can be lifted before the lifting operator returns the same path as its input, that is, $L^{(u)}(p_2) = L^{(u+1)}(p_2)$ for a sufficiently large u . Let U denote the smallest of such values of u , i.e., $U \triangleq \min\{u \in \mathbb{N} : L^{(u)}(p_2) = L^{(u+1)}(p_2)\}$.

If Algorithm 2 fails to provide a valid path, it necessarily fails to find a valid path at all iterations and, in particular, at the U -th iteration. Therefore, to prove the theorem, it suffices to show that the algorithm succeeds if it reaches the U -th iteration, which is the worst case. To this end, suppose that there is a path for UAV-1 that results in a valid (combined) path when UAV-2 follows

$$L^{(U)}(p_2) = \{\mathbf{q}_2[0], L^{(1)}(\mathbf{q}_2[0]), \dots, L^{(U^\uparrow)}(\mathbf{q}_2[0]), \mathbf{q}_2^{(U)}[1], \dots, \mathbf{q}_2^{(U)}[N_U - 2], L^{(U^\downarrow)}(\mathbf{q}_2[N_0 - 1]), \dots, \mathbf{q}_2[N_0 - 1]\}, \quad (13)$$

where $U^\uparrow \triangleq \min\{u \in \mathbb{N} : L^{(u)}(\mathbf{q}_2[0]) = L^{(u+1)}(\mathbf{q}_2[0])\}$, $U^\downarrow \triangleq \min\{u \in \mathbb{N} : L^{(u)}(\mathbf{q}_2[N_0 - 1]) = L^{(u+1)}(\mathbf{q}_2[N_0 - 1])\}$, and $\{L^{(U^\uparrow)}(\mathbf{q}_2[0]), \mathbf{q}_2^{(U)}[1], \dots, \mathbf{q}_2^{(U)}[N_U - 2], L^{(U^\downarrow)}(\mathbf{q}_2[N_0 - 1])\}$ is the shortest path from $L^{(U^\uparrow)}(\mathbf{q}_2[0])$ to $L^{(U^\downarrow)}(\mathbf{q}_2[N_0 - 1])$ in the graph of Sec. IV-A1. Then, there is necessarily a path from a node corresponding to $\mathcal{N}_1[0]$ to a node corresponding to \mathcal{D}_1 in the extended graph constructed from $L^{(U)}(p_2)$. The combined path is, therefore, feasible. Since Algorithm 2 is based on a shortest path algorithm and a feasible path exists, a feasible path will be found. Due to Algorithm 1, $\mathbf{q}_2[N_0 - 1] \in \mathcal{R}(\mathbf{q}_{\text{BS}}, 2r_{\text{CC}} + r_{\text{UE}}^{\min}, r_{\text{CC}} + r_{\text{UE}}^{\min}) \cap \mathcal{R}(\mathbf{q}_{\text{UE}}, r_{\text{UE}}^{\min})$, which implies that this path is also valid. Therefore, to prove the theorem, it suffices to find any path for UAV-1 such that the combined path of both UAVs is feasible, and this path needs not be the one produced by Algorithm 2.

For this reason, the rest of the proof shows that there exists a path for UAV-1 that results in a combined feasible path when UAV-2 follows $L^{(U)}(p_2)$. This amounts to showing that there exists a path for UAV-1 such that, when UAV-2 follows $L^{(U)}(p_2)$, the resulting combined path is valid. This path will be explicitly constructed in such a way that the last point of this path will also be in $\mathcal{R}(\mathbf{q}_{\text{BS}}, 2r_{\text{CC}} + r_{\text{UE}}^{\min}) \cap \mathcal{R}(\mathbf{q}_2[N_0 - 1], r_{\text{CC}} + r_{\text{UE}}^{\min})$, which means that the constructed combined path will be valid so long as it is feasible.

A path will be designed for UAV-1 and the combined path $P \triangleq \{\dot{\mathbf{Q}}[0], \dots, \dot{\mathbf{Q}}[N - 1]\}$ will be shown to be feasible. With $\dot{\mathbf{Q}}[n] = [\dot{\mathbf{q}}_1[n], \dot{\mathbf{q}}_2[n]]$, this means that the following conditions hold:

- C1: The rate between the BS and UAV-1 is at least $2r_{\text{CC}}$, i.e., $c(\mathbf{q}_{\text{BS}}, \dot{\mathbf{q}}_1[n]) \geq 2r_{\text{CC}}$ for all n , and

Proof: See Appendix B. ■

From (19), (22), (25) and Lemma 1, it holds that, $\forall \hat{\mathbf{q}}_2 \in \vec{p}$,

$$\begin{aligned} \|L^{(U^\uparrow)}(\mathbf{q}_2[0]) - \hat{\mathbf{q}}_2\| &\stackrel{(19)}{\leq} \|L^{(U^\uparrow)}(\mathbf{q}_2[0]) - L^{(U^\downarrow)}(\mathbf{q}_2[N_0 - 1])\| \\ &\stackrel{(22)}{\leq} \|L^{(U^\uparrow)}(\mathbf{q}_2[0]) - \bar{\mathbf{q}}_1^*\| + \|L^{(U^\downarrow)}(\mathbf{q}_2[N_0 - 1]) - \bar{\mathbf{q}}_1^*\| \\ &\stackrel{(25)}{\leq} c^{-1}(2r_{CC} + r_{UE}^{\min}) + c^{-1}(r_{CC} + r_{UE}^{\min}) \stackrel{(\text{Lemma 1})}{\leq} c^{-1}(r_{CC}). \end{aligned}$$

Therefore, $c(L^{(U^\uparrow)}(\mathbf{q}_2[0]), \hat{\mathbf{q}}_2) \geq r_{CC}$, which establishes C2.

Part 2: Next, UAV-1 follows a shortest path from $L^{(U^\uparrow)}(\mathbf{q}_2[0])$ to $\bar{\mathbf{q}}_1^*$ in $\bar{\mathcal{F}}_G$ while UAV-2 stays at $L^{(U^\downarrow)}(\mathbf{q}_2[N_0 - 1])$. Since the flight grid is dense enough, there exists a sequence of adjacent grid points $\bar{p} \triangleq \{L^{(U^\uparrow)}(\mathbf{q}_2[0]), \bar{\mathbf{q}}_1^*[1], \bar{\mathbf{q}}_1^*[2], \dots, \bar{\mathbf{q}}_1^*[\bar{N} - 2], \bar{\mathbf{q}}_1^*\}$ that are sufficiently close to the line segment from $L^{(U^\uparrow)}(\mathbf{q}_2[0])$ to $\bar{\mathbf{q}}_1^*$ so that the rate between the BS and UAV-1 on this path will be at least $c(\mathbf{q}_2[0], \bar{\mathbf{q}}_1^*)$. The combined path is then

$$\begin{aligned} \vec{P}_2 \triangleq &\left\{ \left[L^{(U^\uparrow)}(\mathbf{q}_2[0]), L^{(U^\downarrow)}(\mathbf{q}_2[N_0 - 1]) \right], \right. \\ &\left[\bar{\mathbf{q}}_1^*[1], L^{(U^\downarrow)}(\mathbf{q}_2[N_0 - 1]) \right], \dots, \\ &\left. \left[\bar{\mathbf{q}}_1^*[\bar{N} - 2], L^{(U^\downarrow)}(\mathbf{q}_2[N_0 - 1]) \right], \left[\bar{\mathbf{q}}_1^*, L^{(U^\downarrow)}(\mathbf{q}_2[N_0 - 1]) \right] \right\}. \end{aligned} \quad (28)$$

C1: Since \bar{p} is the set of adjacent grid points approximately on the line segment between $L^{(U^\uparrow)}(\mathbf{q}_2[0])$ and $\bar{\mathbf{q}}_1^*$, it holds that, $\forall \hat{\mathbf{q}}_1 \in \bar{p}$,

$$\|L^{(U^\uparrow)}(\mathbf{q}_2[0]) - \hat{\mathbf{q}}_1\| \leq \|L^{(U^\uparrow)}(\mathbf{q}_2[0]) - \bar{\mathbf{q}}_1^*\|. \quad (29)$$

Squaring both sides and adding $\|\mathbf{q}_{BS} - L^{(U^\uparrow)}(\mathbf{q}_2[0])\|^2$ yields

$$\begin{aligned} \|\mathbf{q}_{BS} - L^{(U^\uparrow)}(\mathbf{q}_2[0])\|^2 + \|L^{(U^\uparrow)}(\mathbf{q}_2[0]) - \hat{\mathbf{q}}_1\|^2 \\ \leq \|\mathbf{q}_{BS} - L^{(U^\uparrow)}(\mathbf{q}_2[0])\|^2 + \|L^{(U^\uparrow)}(\mathbf{q}_2[0]) - \bar{\mathbf{q}}_1^*\|^2. \end{aligned} \quad (30)$$

From Pythagoras' theorem, $\forall \hat{\mathbf{q}}_1 \in \bar{p}$, $\|\mathbf{q}_{BS} - \hat{\mathbf{q}}_1\|^2 \leq \|\mathbf{q}_{BS} - \bar{\mathbf{q}}_1^*\|^2$, which in turn implies that

$$c(\mathbf{q}_{BS}, \hat{\mathbf{q}}_1) \geq c(\mathbf{q}_{BS}, \bar{\mathbf{q}}_1^*). \quad (31)$$

Let $\text{proj}(\mathbf{q}) \triangleq [x, y, z_{BS}]^\top$ be the projection of $\mathbf{q} = [x, y, z]^\top$ on the horizontal plane containing the BS. Then, $\text{proj}(\mathbf{q}_1^*) \equiv \text{proj}(\bar{\mathbf{q}}_1^*)$. From Pythagoras' theorem,

$$\|\mathbf{q}_{BS} - \bar{\mathbf{q}}_1^*\|^2 \leq h_{\max}^2 + \|\mathbf{q}_{BS} - \text{proj}(\bar{\mathbf{q}}_1^*)\|^2 \quad (32a)$$

$$= h_{\max}^2 + \|\mathbf{q}_{BS} - \text{proj}(\mathbf{q}_1^*)\|^2 \leq h_{\max}^2 + \|\mathbf{q}_{BS} - \mathbf{q}_1^*\|^2 \quad (32b)$$

$$\stackrel{(21a)}{\leq} h_{\max}^2 + [c^{-1}(2r_{CC} + r_{UE}^{\min})]^2 \stackrel{(16)}{\leq} [c^{-1}(2r_{CC})]^2. \quad (32c)$$

Hence,

$$c(\mathbf{q}_{BS}, \bar{\mathbf{q}}_1^*) \geq 2r_{CC}. \quad (33)$$

From (31) and (33), $\forall \hat{\mathbf{q}}_1 \in \bar{p}$,

$$c(\mathbf{q}_{BS}, \hat{\mathbf{q}}_1) \geq 2r_{CC}, \quad (34)$$

which proves C1.

C2: Since \bar{p} comprises grid points sufficiently close to the line segment between $L^{(U^\uparrow)}(\mathbf{q}_2[0])$ and $\bar{\mathbf{q}}_1^*$, $\forall \hat{\mathbf{q}}_1 \in \bar{p}$,

$$\|\hat{\mathbf{q}}_1 - \bar{\mathbf{q}}_1^*\| \leq \|L^{(U^\uparrow)}(\mathbf{q}_2[0]) - \bar{\mathbf{q}}_1^*\|. \quad (35)$$

From the triangle inequality, $\forall \hat{\mathbf{q}}_1 \in \bar{p}$,

$$\begin{aligned} \|\hat{\mathbf{q}}_1 - L^{(U^\downarrow)}(\mathbf{q}_2[N_0 - 1])\| \\ \leq \|\hat{\mathbf{q}}_1 - \bar{\mathbf{q}}_1^*\| + \|\bar{\mathbf{q}}_1^* - L^{(U^\downarrow)}(\mathbf{q}_2[N_0 - 1])\| \end{aligned} \quad (36a)$$

$$\stackrel{(35)}{\leq} \|L^{(U^\uparrow)}(\mathbf{q}_2[0]) - \bar{\mathbf{q}}_1^*\| + \|\bar{\mathbf{q}}_1^* - L^{(U^\downarrow)}(\mathbf{q}_2[N_0 - 1])\|. \quad (36b)$$

Then, from (36b), (25), and Lemma 1, $\forall \hat{\mathbf{q}}_1 \in \bar{p}$,

$$\begin{aligned} \|\hat{\mathbf{q}}_1 - L^{(U^\downarrow)}(\mathbf{q}_2[N_0 - 1])\| \\ \stackrel{(36b)}{\leq} \|L^{(U^\uparrow)}(\mathbf{q}_2[0]) - \bar{\mathbf{q}}_1^*\| + \|\bar{\mathbf{q}}_1^* - L^{(U^\downarrow)}(\mathbf{q}_2[N_0 - 1])\| \\ \stackrel{(25)}{\leq} c^{-1}(2r_{CC} + r_{UE}^{\min}) + c^{-1}(r_{CC} + r_{UE}^{\min}) \stackrel{\text{Lemma 1}}{\leq} c^{-1}(r_{CC}). \end{aligned}$$

Therefore,

$$c(\hat{\mathbf{q}}_1, L^{(U^\downarrow)}(\mathbf{q}_2[N_0 - 1])) \geq r_{CC}, \quad (38)$$

which proves C2.

Landing subpath (p^\downarrow): The landing path of UAV-2 is $p^\downarrow = \{L^{(U^\downarrow)}(\mathbf{q}_2[N_0 - 1]), L^{(U^\downarrow-1)}(\mathbf{q}_2[N_0 - 1]), \dots, \mathbf{q}_2[N_0 - 1]\}$. Let $U_1^\downarrow \triangleq \min\{u \in \mathbb{N} : L^{(u)}(\mathbf{q}_1^*) = L^{(u+1)}(\mathbf{q}_1^*) \triangleq \bar{\mathbf{q}}_1^*\}$.

If $U^\downarrow \leq U_1^\downarrow$, \mathbf{q}_1^* has a lower altitude than $\mathbf{q}_2[N_0 - 1]$ and $L^{(U_1^\downarrow - U^\downarrow)}(\mathbf{q}_1^*)$ and $\mathbf{q}_2[N_0 - 1]$ are at the same height. The case when $U^\downarrow > U_1^\downarrow$ can be proven similarly. With $U^\downarrow \leq U_1^\downarrow$, the UAVs descend simultaneously following the combined subpath

$$\begin{aligned} P_1^\downarrow \triangleq &\left\{ \left[L^{(U_1^\downarrow)}(\mathbf{q}_1^*), L^{(U^\downarrow)}(\mathbf{q}_2[N_0 - 1]) \right], \right. \\ &\left[L^{(U_1^\downarrow-1)}(\mathbf{q}_1^*), L^{(U^\downarrow-1)}(\mathbf{q}_2[N_0 - 1]) \right], \dots, \\ &\left[L^{(U_1^\downarrow - U^\downarrow + 1)}(\mathbf{q}_1^*), L^{(1)}(\mathbf{q}_2[N_0 - 1]) \right], \\ &\left. \left[L^{(U_1^\downarrow - U^\downarrow)}(\mathbf{q}_1^*), \mathbf{q}_2[N_0 - 1] \right] \right\}. \end{aligned} \quad (39)$$

After that UAV-1 continues its descent while UAV-2 stays at $\mathbf{q}_2[N_0 - 1]$. The second combined subpath is then

$$\begin{aligned} P_2^\downarrow \triangleq &\left\{ \left[L^{(U_1^\downarrow - U^\downarrow)}(\mathbf{q}_1^*), \mathbf{q}_2[N_0 - 1] \right], \right. \\ &\left[L^{(U_1^\downarrow - U^\downarrow - 1)}(\mathbf{q}_1^*), \mathbf{q}_2[N_0 - 1] \right], \dots, \\ &\left. \left[L^{(1)}(\mathbf{q}_1^*), \mathbf{q}_2[N_0 - 1] \right], \left[\mathbf{q}_1^*, \mathbf{q}_2[N_0 - 1] \right] \right\}. \end{aligned} \quad (40)$$

C1: Proving C1 amounts to showing that $c(\mathbf{q}_{BS}, L^{(u)}(\mathbf{q}_1^*)) \geq 2r_{CC}$ for $u = 0, \dots, U_1^\downarrow$. It is easy to see that

$$\begin{aligned} c(\mathbf{q}_{BS}, L^{(u)}(\mathbf{q}_1^*)) &\geq \min \left[c(\mathbf{q}_{BS}, L^{(0)}(\mathbf{q}_1^*)), c(\mathbf{q}_{BS}, L^{(U_1^\downarrow)}(\mathbf{q}_1^*)) \right] \\ &= \min \left[c(\mathbf{q}_{BS}, \mathbf{q}_1^*), c(\mathbf{q}_{BS}, \bar{\mathbf{q}}_1^*) \right]. \end{aligned} \quad (41)$$

From (20), it follows that $c(\mathbf{q}_{BS}, \mathbf{q}_1^*) \geq 2r_{CC} + r_{UE}^{\min} > 2r_{CC}$. On the other hand, from (33), it follows that $c(\mathbf{q}_{BS}, \bar{\mathbf{q}}_1^*) \geq 2r_{CC}$. Hence, C1 is proven for P_1^\downarrow and P_2^\downarrow .

C2: One has, $\forall u = 0, \dots, U^\downarrow$, $\|L^{(U_1^\downarrow - u)}(\mathbf{q}_1^*) - L^{(U^\downarrow - u)}(\mathbf{q}_2[N_0 - 1])\| \leq \|\mathbf{q}_1^* - \mathbf{q}_2[N_0 - 1]\|$, then,

$$\begin{aligned} c(L^{(U_1^\downarrow - u)}(\mathbf{q}_1^*), L^{(U^\downarrow - u)}(\mathbf{q}_2[N_0 - 1])) &\geq c(\mathbf{q}_1^*, \mathbf{q}_2[N_0 - 1]) \\ &\stackrel{(20)}{\geq} r_{CC} + r_{UE}^{\min} > r_{CC}, \end{aligned} \quad (42)$$

which proves C2 for P_1^\downarrow .

In P_2^\downarrow , UAV-1 descends from $L^{(U_1^\downarrow - U^\downarrow)}(\mathbf{q}_1^*)$ to \mathbf{q}_1^* while UAV-2 stays at $\mathbf{q}_2[N_0 - 1]$. Start by noting that $L^{(u)}(\mathbf{q}_1^*)$ is between \mathbf{q}_1^* and $L^{(U_1^\downarrow - U^\downarrow)}(\mathbf{q}_1^*)$, $\forall u = 0, \dots, U_1^\downarrow - U^\downarrow$, which means that

$$\|L^{(u)}(\mathbf{q}_1^*) - L^{(U_1^\downarrow - U^\downarrow)}(\mathbf{q}_1^*)\|^2 \leq \|\mathbf{q}_1^* - L^{(U_1^\downarrow - U^\downarrow)}(\mathbf{q}_1^*)\|^2. \quad (43)$$

From Pythagoras' theorem,

$$\begin{aligned} \|L^{(u)}(\mathbf{q}_1^*) - \mathbf{q}_2[N_0 - 1]\|^2 &= \|L^{(u)}(\mathbf{q}_1^*) - L^{(U_1^\downarrow - U^\downarrow)}(\mathbf{q}_1^*)\|^2 \\ &+ \|L^{(U_1^\downarrow - U^\downarrow)}(\mathbf{q}_1^*) - \mathbf{q}_2[N_0 - 1]\|^2 \\ &\stackrel{(43)}{\leq} \|\mathbf{q}_1^* - L^{(U_1^\downarrow - U^\downarrow)}(\mathbf{q}_1^*)\|^2 + \|L^{(U_1^\downarrow - U^\downarrow)}(\mathbf{q}_1^*) - \mathbf{q}_2[N_0 - 1]\|^2 \\ &= \|\mathbf{q}_1^* - \mathbf{q}_2[N_0 - 1]\|^2. \end{aligned} \quad (44)$$

It follows that $c(L^{(u)}(\mathbf{q}_1^*), \mathbf{q}_2[N_0 - 1]) \geq c(\mathbf{q}_1^*, \mathbf{q}_2[N_0 - 1]) \geq r_{CC} + r_{UE}^{\min} > r_{CC}$, where the second inequality follows from (20). This proves C2 for P_2^\downarrow .

The case when $U^\downarrow > U_1^\downarrow$, i.e., \mathbf{q}_1^* has a higher altitude than $\mathbf{q}_2[N_0 - 1]$, can be proven similarly.

Finally, it is clear that if no lifting and waiting steps are required in Algorithm 2, then the obtained path is optimal among all paths on \mathcal{F}_G because in no other path can UAV-2 fly from $\mathbf{q}_2[0]$ to \mathcal{D}_2 in a shorter time. Else, this would contradict the fact that Algorithm 1 returns the shortest path.

APPENDIX B PROOF OF LEMMA 1

Let $a \triangleq r_{CC}/B > 0$ and $\ell \triangleq r_{UE}^{\min}/r_{CC} \geq 4$. Then $(2r_{CC} + r_{UE}^{\min})/B = (2 + \ell)r_{CC}/B = (\ell + 2)a$ and $(r_{CC} + r_{UE}^{\min})/B = (1 + \ell)r_{CC}/B = (\ell + 1)a$. From (3), it follows that the inverse of $c(d)$ is

$$c^{-1}(r) \triangleq \left(\frac{A}{2^{r/B} - 1} \right)^{1/2}. \quad (45a)$$

As a result,

$$\begin{aligned} c^{-1}(2r_{CC} + r_{UE}^{\min}) + c^{-1}(r_{CC} + r_{UE}^{\min}) \\ = \left(\frac{A}{2^{(\ell+2)a} - 1} \right)^{1/2} + \left(\frac{A}{2^{(\ell+1)a} - 1} \right)^{1/2}. \end{aligned} \quad (46)$$

Since $a > 0$ and $\ell \geq 4$, one has that $(\ell + 2)a > (\ell + 1)a > \ell a$, which in turn implies

$$\left(\frac{A}{2^{(\ell+2)a} - 1} \right)^{1/2} < \left(\frac{A}{2^{\ell a} - 1} \right)^{1/2}, \quad \text{or,} \quad (47a)$$

$$\left(\frac{A}{2^{(\ell+1)a} - 1} \right)^{1/2} < \left(\frac{A}{2^{\ell a} - 1} \right)^{1/2}. \quad (47b)$$

It follows that

$$\begin{aligned} \left(\frac{A}{2^{(\ell+2)a} - 1} \right)^{1/2} + \left(\frac{A}{2^{(\ell+1)a} - 1} \right)^{1/2} \\ < 2 \left(\frac{A}{2^{\ell a} - 1} \right)^{1/2} \stackrel{(\ell \geq 4)}{\leq} 2 \left(\frac{A}{2^{4a} - 1} \right)^{1/2}. \end{aligned} \quad (48)$$

With $a > 0$, it holds that $2^{2a} + 1 \geq 2^a + 1 \geq 2$, which yields

$$\frac{4A}{(2^a + 1)(2^{2a} + 1)} \leq \frac{4A}{2 \cdot 2} = A. \quad (49a)$$

Multiplying both sides by $1/(2^a - 1)$ and applying simple manipulations produces

$$2 \left(\frac{A}{2^{4a} - 1} \right)^{1/2} \leq \left(\frac{A}{2^a - 1} \right)^{1/2}. \quad (50a)$$

Indeed,

$$\left(\frac{A}{2^a - 1} \right)^{1/2} = c^{-1}(r_{CC}). \quad (51)$$

From (46), (48), (50a), and (51), it follows that

$$c^{-1}(2r_{CC} + r_{UE}^{\min}) + c^{-1}(r_{CC} + r_{UE}^{\min}) < c^{-1}(r_{CC}), \quad (52a)$$

which concludes the proof.

APPENDIX C PROOF OF THEOREM 2

This proof follows a similar logic to the one in the proof of Theorem 1. Algorithm 5 fails iff there is no path for UAV-1 that results in a feasible combined path at all iterations, in particular at the U -th iteration, where $U \triangleq \min\{u : \bar{L}^{(u)}(p_2) = \bar{L}^{(u+1)}(p_2)\}$. Therefore, it suffices to show that there exists a path for UAV-1 (not necessarily the one produced by Algorithm 5) that results in a feasible combined path when UAV-2 follows $\bar{L}^{(U)}(p_2)$. To this end, a path will be designed for UAV-1 and the combined path $P \triangleq \{\dot{\mathbf{Q}}[0], \dots, \dot{\mathbf{Q}}[N_{UE} - 1]\}$, where $\dot{\mathbf{Q}}[n] \triangleq [\dot{\mathbf{q}}_1[n], \dot{\mathbf{q}}_2[n]]$ and $\{\dot{\mathbf{q}}_2[0], \dots, \dot{\mathbf{q}}_2[N_{UE} - 1]\} = \bar{L}^{(U)}(p_2)$ will be shown to be feasible. This means that the following conditions hold:

- C1: The rate between the BS and UAV-1 is at least $2r_{CC}$, i.e., $c(\mathbf{q}_{BS}, \dot{\mathbf{q}}_1[n]) \geq 2r_{CC}$ for all n , and
- C2: The rate from UAV-1 to UAV-2 is at least r_{CC} , i.e., $c(\dot{\mathbf{q}}_1[n], \dot{\mathbf{q}}_2[n]) \geq r_{CC}$ for all n .

To simplify the exposition, the path $\bar{L}^{(U)}(p_2)$ will be separated into the following subpaths:

$$p^\uparrow \triangleq \{\mathbf{q}_2[0], L^{(1)}(\mathbf{q}_2[0]), \dots, L^{(u_{\max}^\uparrow)}(\mathbf{q}_2[0])\}, \quad (53a)$$

$$\vec{p} \triangleq \{L^{(u_{\max}^\uparrow)}(\mathbf{q}_2[0]), \bar{\mathbf{q}}_2[1], \dots, \bar{\mathbf{q}}_2[N_{UE} - u_{\max}^\uparrow - 1]\}. \quad (53b)$$

For each of them, a path will be designed for UAV-1 and the resulting combined path will be shown to satisfy C1 and C2. The designed path is illustrated in Fig. 12.

Take-off subpaths (p^\uparrow) In the considered combined path, when UAV-2 follows p^\uparrow , UAV-1 follows p^\uparrow as well. Recall that the minimum separation between the UAVs was disregarded in (4) for simplicity. Thus, the combined path of UAV-1 and UAV-2 is given by

$$\begin{aligned} P^\uparrow \triangleq \left\{ [\mathbf{q}_2[0], \mathbf{q}_2[0]], [L^{(1)}(\mathbf{q}_2[0]), L^{(1)}(\mathbf{q}_2[0])], \dots, \right. \\ \left. [L^{(u_{\max}^\uparrow)}(\mathbf{q}_2[0]), L^{(u_{\max}^\uparrow)}(\mathbf{q}_2[0])] \right\}. \end{aligned} \quad (54)$$

C1: By hypothesis, $h_{\max} \leq c^{-1}(2r_{CC})$. Thus, since $\mathbf{q}_2[0] = \mathbf{q}_{BS}$, $\forall \dot{\mathbf{q}}_1 \in p^\uparrow$, it follows that $\|\mathbf{q}_{BS} - \dot{\mathbf{q}}_1\| \leq \|\mathbf{q}_{BS} - L^{(u_{\max}^\uparrow)}(\mathbf{q}_2[0])\| \leq h_{\max} \leq c^{-1}(2r_{CC})$. Noting that c is a decreasing function of the distance yields

$$c(\mathbf{q}_{BS}, \dot{\mathbf{q}}_1) \geq c(\mathbf{q}_{BS}, L^{(u_{\max}^\uparrow)}(\mathbf{q}_2[0])) \geq 2r_{CC}, \quad (55a)$$

which establishes C1.

C2: trivial.

Top subpath (\vec{p}): In the considered combined path, when UAV-2 follows \vec{p} , UAV-1 stays at $L^{(u_{\max}^\uparrow)}(\mathbf{q}_2[0])$. This results in the following combined path

$$P^\uparrow \triangleq \left\{ \left[L^{(u_{\max}^\uparrow)}(\mathbf{q}_2[0]), L^{(u_{\max}^\uparrow)}(\mathbf{q}_2[0]) \right], \left[L^{(u_{\max}^\uparrow)}(\mathbf{q}_2[0]), \bar{\mathbf{q}}_2[1] \right], \dots, \left[L^{(u_{\max}^\uparrow)}(\mathbf{q}_2[0]), \bar{\mathbf{q}}_2[N_{\text{UE}} - u_{\max}^\uparrow - 1] \right] \right\}. \quad (56)$$

C1: shown previously.

C2: By definition of U , $[0, 0, 1]\dot{\mathbf{q}}_2 = h_{\max}, \forall \dot{\mathbf{q}}_2 \in \vec{p}$. Also, $\mathbf{q}_2[0] = \mathbf{q}_{\text{BS}}$. This means that $\forall \dot{\mathbf{q}}_2 \in \vec{p}, \|L^{(u_{\max}^\uparrow)}(\mathbf{q}_2[0]) - \dot{\mathbf{q}}_2\| \leq d_{c,\min} \leq c^{-1}(r_{\text{CC}})$. Then $c(L^{(u_{\max}^\uparrow)}(\mathbf{q}_2[0]), \dot{\mathbf{q}}_2) \geq r_{\text{CC}}, \forall \dot{\mathbf{q}}_2 \in \vec{p}$.

APPENDIX D BENCHMARK 4

In this benchmark, for every N_{replan} time steps, the planner is given the next N_{known} locations of the user, $N_{\text{replan}} \leq N_{\text{known}}$. The following steps will be iteratively implemented at time steps $nN_{\text{replan}}, n = 0, 1, \dots$

- S1: The planner uses the algorithms in Sec. IV-A to plan a path for the UAVs to the nearest grid points where they can serve
- All of the next N_{known} locations of the user.
 - If such grid points do not exist, the planner plans a path to the nearest grid points where the UAVs can serve the last $(N_{\text{known}} - 1)$ known locations of the user, i.e., $\mathbf{q}_{\text{UE}}[nN_{\text{replan}} + i], i = 1, \dots, N_{\text{known}} - 1$, and so on.
 - In the most extreme case when the planner cannot find grid points to simultaneously guarantee r_{UE}^{\min} to multiple locations of the user, the planner plans a path to the nearest grid point where the UAVs can serve the last known location of the user, i.e., $\mathbf{q}_{\text{UE}}[nN_{\text{replan}} + N_{\text{known}} - 1]$.
- S2: If the length of the path obtained in Step 1 is less than N_{replan} , the last configuration point of the path is repeated until the length of the path is N_{replan} . If the length of the path obtained in Step 1 is greater than N_{replan} , only the first N_{replan} configuration points of the path are kept.
- S3: The last configuration point of the path obtained in Step 2 provides the start locations of the UAVs in the next iteration, i.e., at time step $(n + 1)N_{\text{replan}}$.